ADVANCED FUNCTIONAL MATERIALS
www.afm-journal.de

Recent Advances in Shape Memory Polymers: Multifunctional Materials, Multiscale Structures, and Applications

Lan Luo, Fenghua Zhang, Linlin Wang, Yanju Liu, and Jinsong Leng**

Shape memory polymers (SMPs) are one of the primary directions in the development of modern high-tech new materials, which are integrated with sensing, actuation, information processing, and autonomous deformation. Here, multifunctional shape memory polymers are focused and a detailed introduction to the characteristics of self-deformation, self-sensing, self-healing, and self-learning is provided. Integrating with other functional materials to form shape memory polymer composites (SMPC), designing and controlling the material structure and organization at the microscale, thereby achieving more precise and controllable shape memory effects and expanding the potential of material applications. Ultimately, it is shown that SMPs and their composites have a wide range of fascinating applications in the fields of robotics, smart clothing, smart textiles, biomedical devices, and wearable technology. SMPs will thus continue to play a significant role in future deeper exploration.

1. Introduction

Since the notion of smart materials was initially put forward in the latter part of the 1980s, the application of smart materials has penetrated the important fields of artificial intelligence, biomedicine, aerospace, flexible electronics, robotics, smart manufacturing, etc., and has become the cornerstone of modern industrial development. Smart composites refer to a class of new materials that can make active responses under external excitation, with the functions of self-sensing, self-driving, self-healing, etc. It is the product of the intersection of multiple disciplines, such as mechanics, physics, materials, chemistry, mechanics, and microelectronics.[1] Smart materials and smart structures are machinable or intelligent structural systems that integrate sensing, control, and drive (actuation) functions. Shape memory polymers (SMPs) refer to a category of polymer materials that possess the unique ability to recover to their permanent shape and dimensions when subjected to specific external conditions after being deformed and fixated (e.g., external stimuli such as heat,[2] electricity,[3] light,[4] magnetism,[5] or solution).[6]. SMPs are characterized by variable stiffness, programmable deformation, composability, large deformations, and easy molding. Shape memory polymers include thermosetting resins and thermoplastic resins, such as epoxy resin (EP), cyanate ester (CE), polyurethane (PU), polyimide (PI), polystyrene (PS), polylactic acid (PLA), polycaprolactone (PCL), etc. Shape memory polymer composites (SMPCs) can be fabricated by incorporating conductive particles such as carbon nanotubes and nanogold, which are responsive to electrical and optical excitations. At present, SMPCs have been widely developed in the fields of domains engineering, biomedicine, flexible electronics, and soft robotics, etc. The unique properties of smart composites will lead the new direction of development in aerospace, new aircraft, intelligent manufacturing, biomedicine, and other fields, and provide the material foundation and guarantee for constructing an intelligent society in the future.

In aerospace, it is advantageous to have a high compression ratio as it helps minimize storage space and provides the necessary driving force for intelligent bionics.[7] Also, it is widely used in various fields, such as biomedical, where it is regarded as a promising technology.[8] In the past few years, SMPs have been increasingly penetrating the aerospace, industrial, and civil fields, as well as entering into other emerging industries. This paper discusses a type of smart material known as SMPs, which can exhibit various properties under various external stimuli. We highlight the connection between molecular design, macroscopic performance, multifunctionality, and applications while summarizing the most recent developments in the field. Bidirectional shape memory effects, numerous forms, and multifunctional SMPs are advancing to fulfill a variety of applications for novel materials. High-performance SMPs are breaking new ground in a variety of applications thanks to their strength, toughness, and

L. Luo, F. Zhang, L. Wang, J. Leng
Centre for Composite Materials and Structures
Harbin Institute of Technology (HIT)
Harbin 150080, P. R. China
E-mail: fhzhang_hit@163.com; lengjs@hit.edu.cn
Y. Liu
Department of Astronautical Science and Mechanics
Harbin Institute of Technology (HIT)
Harbin 150001, P. R. China

The ORCID identification number(s) for the author(s) of this article can be found under https://doi.org/10.1002/adfm.202312036

[Correction added on January 2, 2024, after first online publication: Fenghua Zhang was assigned corresponding author in this version.]

DOI: 10.1002/adfm.202312036

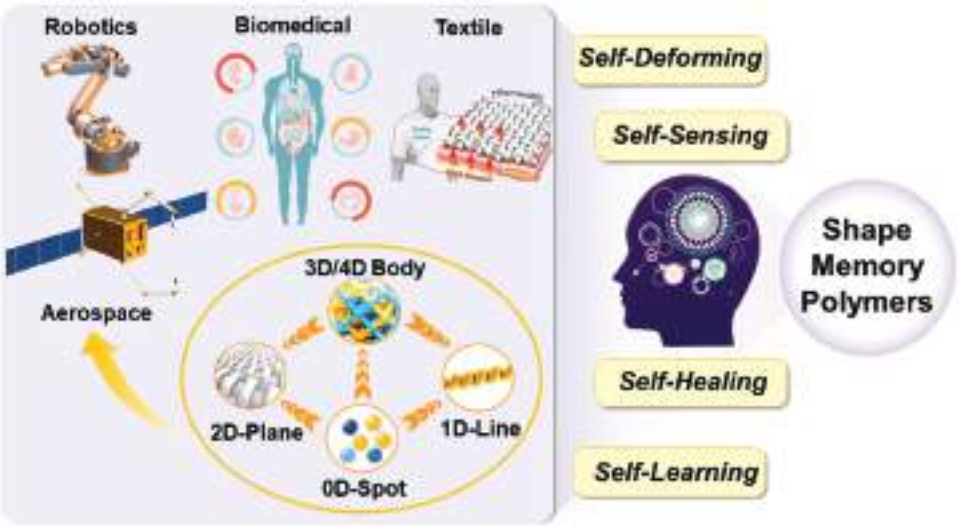

Figure 1. Scheme of the shape memory polymers: mechanism, actuation methods, and applications.

heat resistance. Future smart devices in various scientific and technological disciplines have a lot of potential thanks to SMPs.

In this work, we review a class of intelligent materials called SMPs. We aim to comprehensively review the latest developments in molecular design, with a focus on introducing multifunctional SMPs, multiscale SMPCs, and their applications. We begin with a discussion of the fundamental theory underlying smart composite materials before delving deeply into the areas of study for thermoset shape memory polymers and their thermoplastic shape memory mechanism, as shown in **Figure 1**. In the past decade, SMP's efforts in various fields have increased due to its variable stiffness and active deformation that give materials self-deformation and self-sensing functions. Self-healing based on SMPs can meet the advantages of damage repair and life extension and has made substantial progress. SMP has also gradually combined computer science with the development of artificial intelligence to reduce time and resources greatly. SMP has potential applications in various fields, such as aerospace, biomedicine, robotics, and smart textiles, and their future development paths. We look at the current state of smart composite applications in industries like aircraft, robotics, medicinal devices, and smart textiles, as well as the future paths for their advancement.

2. Mechanism of Shape Memory Polymers

The shape memory mechanism of unidirectional SMPs is the foundation for understanding all SMP deformation processes. Taking thermally triggered dual-SMP as an example, we explain its deformation mechanism from the perspectives of strain elasticity and free energy. Due to the presence of two largely incompatible phases in the material, including a reversible phase that can change with temperature from a glassy state to a rubbery state and a fixed phase that holds the sample's initial shape, the material exhibits shape memory, as shown in **Figure 2**. Depending on the different crosslinking methods of the fixed phase, SMP can be classified into two categories: thermosetting and thermoplastic.[9] The stable polymer network and the reversible switch are two distinct sections of the polymer that give rise to the shape memory effect (SME) of SMP. The stable polymer network is formed by molecular entanglement, crystalline phase, chemical crosslinking, or interpenetrating network,[10] determining the permanent shape of the polymer, while the reversible switch is composed of crystalline-to-amorphous transitions,[11] glass transitions,[12] anisotropy/isotropy conversion,[13] reversible chemical crosslinking[14] or supramolecular structure association/dissociation playing a role in fixing temporary shapes.[15]

2.1. Chemically Crosslinked

A thermosetting SMP is referred to as a fixed phase that possesses a chemically crosslinked structure. The crosslinking points are connected by chemical covalent bonds, which cannot be disrupted by physical means, therefore preventing remolding through melting.[16] The fixed phase can exist in the crystalline or glassy state, while the reversible phase refers to the crystalline state or glassy state of the polymer. When the temperature rises to the melting point of the crystalline phase, the crystalline state disappears or the glassy state transitions into the rubbery state. Under the influence of external forces, the material undergoes elongation, causing directional rearrangement of the molecular chains, which must stretch along the direction of the external force field. When the desired shape is reached, cooling the material allows the reversible phase to enter the glassy or crystalline state, freezing the molecular chains and solidifying the material into a stable solid. Additionally, due to the hindrance provided by the crosslinking, intermolecular sliding is restricted. When the deformed solid is reheated to the rubbery state, thermal motion causes the molecular chains to disorder, thus restoring the original state and generating a recovery force. As a result, the deformed solid can recover its original shape, completing one cycle of shape memory. This mechanism is illustrated in the figure. Thermosetting SMPs exhibit relatively higher shape recovery stress and are more

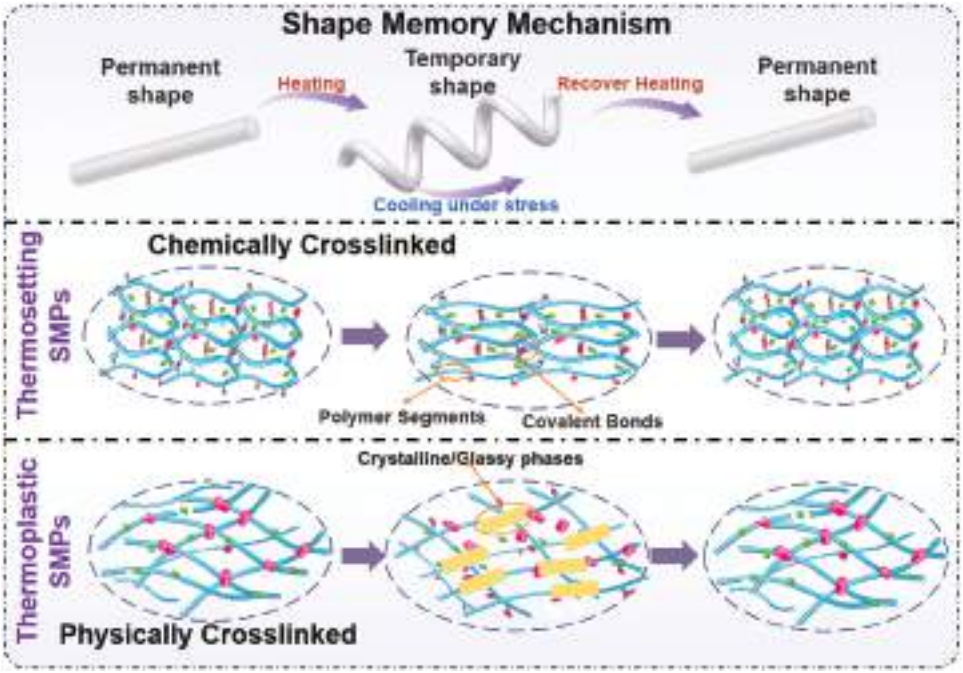

Figure 2. Shape memory mechanism schematic diagram.

suitable for the fabrication of actuators, but they cannot be further processed.

2.2. Physically Crosslinked

A thermoplastic SMP is referred to as a fixed phase that possesses a physical crosslinked structure. The crosslinking points are formed by partial crystalline structures, entanglement of ultrahigh molecular chains, etc. These polymers can be dissolved in specific solvents or melted and reconfigured. The fixed phase with a physical crosslinked structure can be either in a crystalline or glassy state, but its transition temperature must be higher than that of the reversible phase. The reversible phase's molecular chain motion intensifies and changes from the glassy state to the rubbery state when the temperature climbs above its transition temperature. To correct the shape deformation at this stage, an external force is applied and sustained while cooling. The relaxed reversible phase segments are released from their alignment under the recovery stress of the fixed phase as the temperature gradually approaches thermodynamic equilibrium when it rises above the transition temperature once more. The fixed phase of thermoplastic SMPs can also be formed by physically entangled crosslinking points, such as in high molecular weight polyethylene. These polymers exhibit excellent stretchability and reprocessability, but the irreversible chain segment slip can lead to poor shape memory effects.

3. Multifunctional Shape Memory Polymers

SMPs are a class of smart materials with numerous uses that, when triggered by outside stimuli, can regain their original shape from a temporary shape. SMPs can achieve controlled shape adjustment thanks to their adaptability, which offers flexibility and customizability in a variety of settings and applications. They can perceive changes in the surrounding environment and produce corresponding responses. For example, they can trigger changes in shape or function through changes in factors such as temperature, pressure, and humidity, thereby achieving intelligence and responsiveness in practical applications. In addition, self-healing SMPs can repair themselves when the material is damaged or worn, extending their service life and improving stability. Finally, SMPs are gradually developing toward self-learning. This self-learning ability provides possibilities for the optimization and further innovation of materials, promoting research and development in the field of smart materials, as shown in **Figure 3**.

3.1. Self-Deforming

The self-deforming behavior of SMP is influenced by various factors, and the different properties of materials affect their deformation behavior, such as mechanical properties, thermal properties, etc. The micro molecular structure of a material determines its properties, such as crosslinking density, network structure, molecular arrangement, etc. The self-deforming behavior of SMP brings more flexible, intelligent, and efficient solutions in fields such as aerospace, medical devices, smart textiles, and micro devices, with broad application prospects and market potential. In 2016, Hu et al. created a human cartilage-like hydrogel co-polymer using two types of chemical bonding, dynamic and stable. The preprogramming of the material was achieved by adjusting key parameters such as the position, strength, and quantity of chemical bonds,[17] as shown in **Figure 4a**.

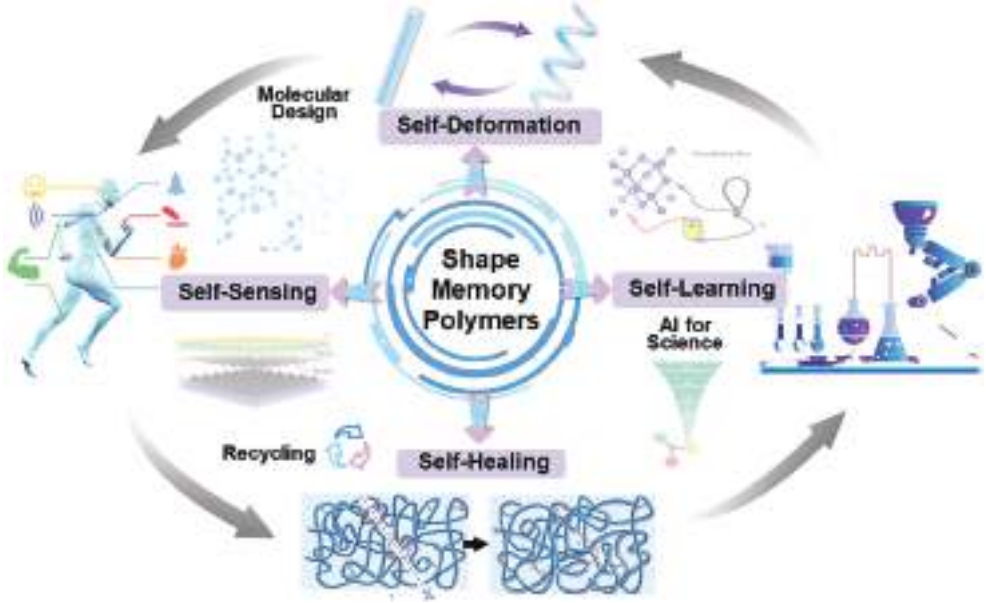

Figure 3. Classification and introduction of smart materials.

The team reported that they have successfully controlled the morphological changes of materials, enabling them to occur within hours, minutes, or seconds. They demonstrated this effect by preparing a flower in which different petals unfold sequentially, mimicking the natural state. The research team believes that this material can be applied to drug delivery inside the human body. The smart material can encapsulate drugs and deliver them to specific locations, and then undergo shape transformation based on pre-programming, enabling drug release. Additionally, Xie et al. observed that programming at high temperatures results in faster hydrogen bond exchange rates, leading to partial chain relaxation and a decrease in entropy driving force within the system. As a result, the spontaneous recovery rate at room temperature is slower. Conversely, programming at low temperatures slows down hydrogen bond exchange rates, while increasing the entropy driving force. This leads to a faster recovery rate at room temperature.[18] Due to the time-temperature equivalence, controlling the programming time can also result in different entropy-driving states, as shown in Figure 4b,c. In conclusion, by controlling the programming time and temperature, spontaneous sequential deformation behavior can be achieved. Subsequently, they discovered a water-based photocurable resin that exhibits a naturally triggered, programmable recovery initiation in the form of SMPs.[19] Interestingly, the material exhibits a "delayed" recovery curve in ambient temperature water, with the recovery appearing to initiate after 10 min (Figure 4d). The programming time ranges from 1 to 1440 min, with the tonnage increasing from 1 to 24 min. The recovery speed decreases with longer programming times, but in all cases, nearly complete recovery is achieved. Luo et al. achieved tunable shape memory epoxy resins (SMEPs) using a series of epoxy monomers with different functionalities through a topological cross-linking network and preliminarily explored the potential application of SMP with high toughness and self-deformation characteristics in the field of artificial muscles (Figure 4e).[20]

3.2. Self-Sensing

Coextrusion 4D printing (CE-4DP), a method suggested by Zhou et al., incorporates continuous metal fibers into thermoplastic SMPs.[22] Establishing a direct heating path through electrical heating in the polymer matrix increased the heating rate of the composite material by 70 times (**Figure** 5a). This allowed for selectively and sequentially heating the SMPC, resulting in precise and programmable deformation, which was employed for self-sensing in shape memory deformation. Tactile sensors made with 4D printing will have previously unheard-of skills including self-perception of motion, environmental adaptation, and self-healing. A multimaterial extrusion method that combines PU in forked electrodes and nano carbon black/polylactic acid composites was used to create a 4D-printed sensor (4DPS) with a distinctive coplanar design, as shown in Figure 5b.[23] Zhu et al. discovered a semicrystalline dynamic ion gel (SDIG) that possesses dual functionalities of environmental sensing and shape memory. This gel has been successfully utilized to mimic biological systems.[24] In the design of semicrystalline dynamic ion gels, the crystalline domains originate from hydrophobic interactions between long alkyl side chains of BeMA (butyl methacrylate), providing dynamic phase transition and shape memory functionalities, as shown in Figure 5c.

Cord-driven continuum robots (CDCRs) are highly important soft robots characterized by their lightweight structure, safety, and high degrees of freedom. They can undergo large-scale bending, twisting, and other deformations based on their inherent flexibility and stretchability, enabling them to work effectively in narrow and complex environments. The lack of adhesive mechanisms greatly limits the motion of soft robots and makes them prone to delamination, which renders rigid sensors unsuitable for integration. However, flexible self-perceptive skin-like water gel sensors, made of ion-conductive polyacrylamide/alginates/nanoclay composite hydrogels, have been

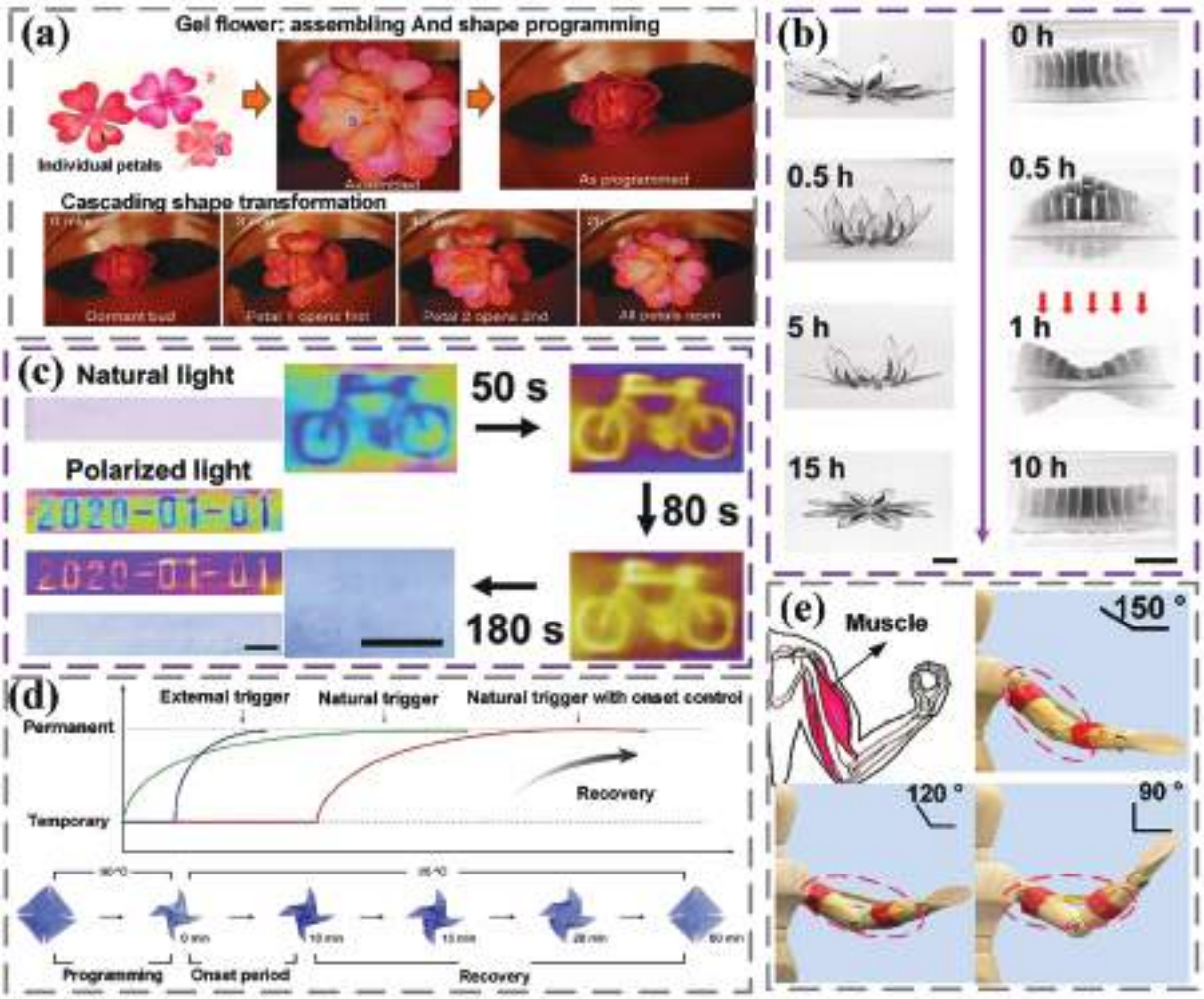

Figure 4. a) The different "petals" of the smart material flower unfold sequentially, mimicking the natural state. Reproduced with permission.[17] Copyright 2016, Nature. b,c) Intricately designed autonomous morphing paths based on cut and draw patterns. Reproduced with permission.[18] Copyright 2021, Wiley-VCH. d) By controlling the programming temperature and time of each part, 4D printing with spontaneous sequential deformation is achieved. Reproduced with permission.[19] Copyright 2023,Nature. e) Deformable shape memory epoxy resin is used for artificial muscles. Reproduced with permission.[21] Copyright 2021, Springer.

developed to enable flexible self-perception in CDCRs.[25] A closed-loop control system was developed to further mimic the sensory system of humans and regulate the bending of CDCR (continuum-driven cable-rod) systems (Figure 5d). He et al. proposed a strategy for soft robots, where the drive and strain sensing are coupled within a homogeneous material. The substance is made up of light-absorbing conductive polymer polypyrrole (PPy) and nanostructured thermoresponsive hydrogel poly(N-isopropylacrylamide) (PNIPAAm), which together create an interpenetrating dual network structure. This strategy offers novel insights into the design of soft robots, enabling them to adapt to complex environments and task requirements. In combination with closed-loop control systems, the soft robots can achieve precise motion control and sensory feedback, enhancing their stability and reliability in operation (Figure 5e).[26] This construction gives the material piezoresistivity and photo/thermoresponsiveness, enabling remote-triggered drive and localized strain detection.

3.3. Self-Healing

Microcracks may develop inside the material under severe settings, and fatigue degradation may finally result in material failure. As a result, the importance of self-healing materials has increased. Restoring release force can be employed in conjunction with shape memory performance to hasten fracture healing. different self-healing systems can be introduced into the polymer matrix to fix cracks of various sizes, as shown in **Figure 6**a.

Larger cracks can be repaired using microvascular and microcapsule procedures, which are permanent fixes that fall under the category of external repair treatments. Excellent SMP effects can also be observed in the EMSP/PCL composite material. Dynamic covalent chemistry enables the repair of irreparable crosslinked polymers. Unlike the external self-healing concept, intrinsic self-healing results from dynamic covalent bond topological alterations at high temperatures. It can be fixed several times and is appropriate for tiny microcracks. Through the

Figure 5. a) Electrically driven shape memory deformation for CMF@PEEK composites. Reproduced with permission.[22] Copyright 2022, Elsevier. b) 4D printing tactile sensor with tunable sensing range. Reproduced with permission.[23] Copyright 2023. c) The ionogel was used to mimic the flower blossoming process. Reproduced with permission.[24] Copyright 2022, American Chemical Society. d) Flexible skin like self-sensing hydrogel sensor. Reproduced with permission.[25] Copyright 2022, Wiley-VCH. e) Cable-driven continuum robot perception using skin-like hydrogel sensors. Reproduced with permission.[26] Copyright 2021, Elsevier.

synergistic effect of hydrogen bonding and dynamic covalent bond, as well as a graded energy dissipation mechanism, Wong et al. created PU elastomers with exceptional mechanical capabilities and shape memory-assisted self-healing properties, as shown in Figure 6b.[27] By adjusting the ratio of metal ion coordination bonds to hydrogen bonds, a series of high-strength and tough elastomeric materials have been obtained. Among them, the tensile strength of the optimized elastomer reaches 76.37 MPa, and the fracture elongation is 839.10%. Metal-organic polyhedra (MOPs) are a novel class of molecular containers/reactors formed by the coordination of metal ions and organic ligands. They could be used in fields such as separation, catalysis, energy storage, and biomedicine. Zhang et al. successfully prepared a multifunctional hypercrosslinked MOP polymer material using a bottom-up approach of macromolecular monomer coordination crosslinking.[28] In addition, the polymer solution of CHMOP can be used as 3D printing ink to achieve the fabrication of complex shapes (Figure 6c). An illustration would be printing the "NKU" pattern at room temperature. Under near-infrared light and direct heating, the dynamic oxime-ester bonds and hydrogen bonds give the printing material self-healing characteristics. A humanoid robot was printed to show the possibility of shape memory recovery in 4D printing. The shape memory recovery can be successfully initiated by near-infrared irradiation or direct heating. Due to their superior mechanical qualities, thermosetting epoxy resins are frequently employed in advanced composite materials, coatings, adhesives, and electronic packaging. Therefore, it is highly desired to develop thermosetting epoxy resins that may be recycled and reprocessed. A new cyclotriphosphazene-based amine curing agent (HVPA)

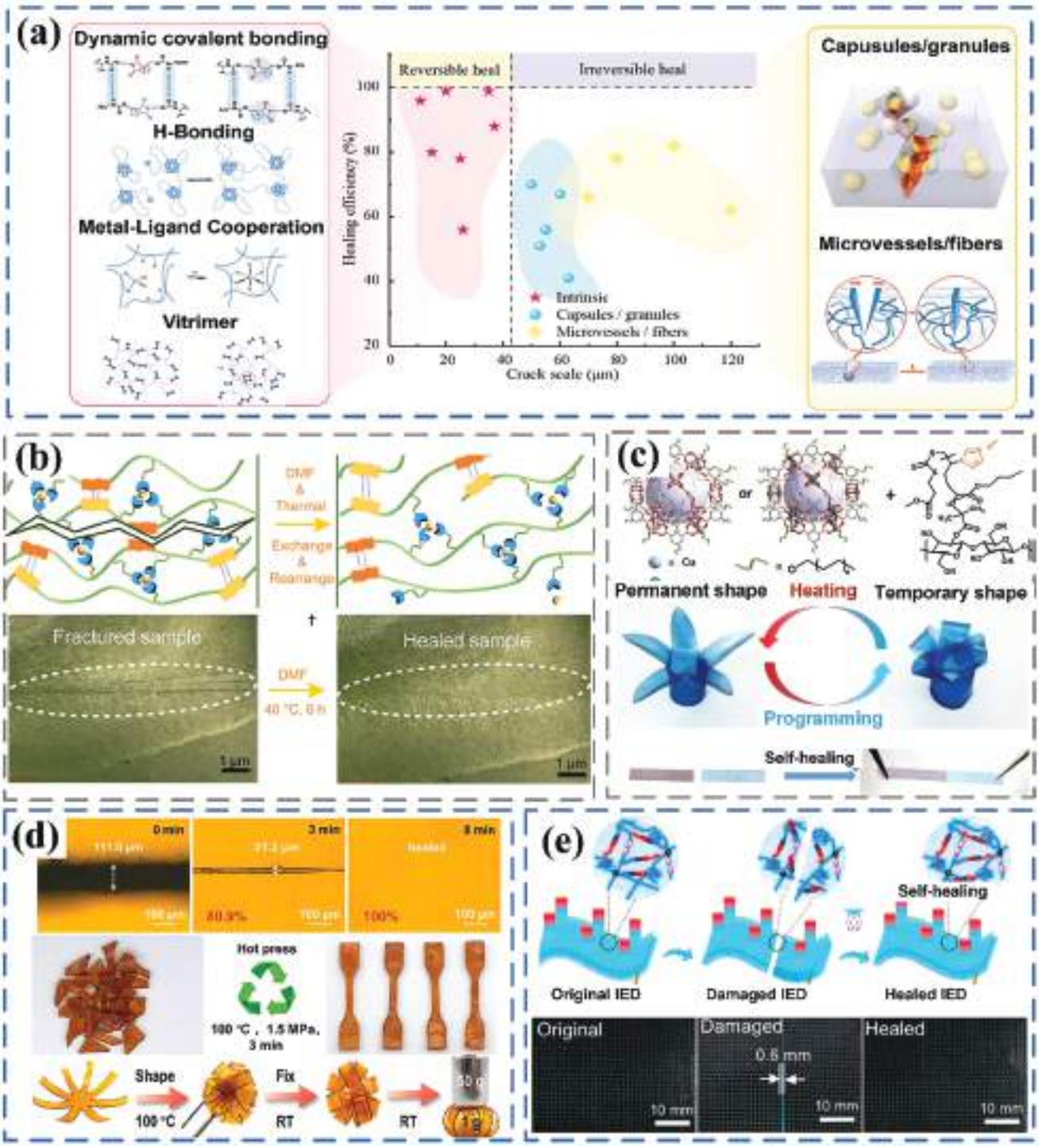

Figure 6. a) Comparison of self-healing efficiency under different self-healing methods; b) Polyurethane urea elastomer with shape memory-assisted self-healing properties. Reproduced with permission.[27] Copyright 2023, Nature. c) Demonstration of the shape memory and self-healing behavior of sample. Reproduced with permission.[28] Copyright 2022. Wiley-VCH. d) Optical microscope photos taken by HVPA/GDE at different self-healing times and 100 °C, and their shape memory behavior. Reproduced with permission.[29] Copyright 2022, Elsevier. e) Wearable and detachable capabilities based on self-healing capabilities. Reproduced with permission.[30] Copyright 2022, American Chemical Society.

containing dynamic imine bonds was produced utilizing bio-based vanillin as the starting material (Figure 6d).[29] HVPA/GDE has a lot of imine bonds, which makes it self-healing, shape-memory, simple to reprocess, and somewhat degradable. This research offers a fresh method for creating thermosetting epoxy resin composites with several uses and good performance. You et al. have developed an integrated triboelectric nanogenerator (TENG) with reprogrammable, self-healing, and wearable properties, referred to as an integrated electronic device (IED). Two PCLUSe films were sequentially delivered to the beating heart of a dog via a 10 mm diameter needle, where they were assembled in situ into a larger film (Figure 6e).[30] The electronic memory effect is achieved through the microscale shape memory characteristics, enabling the reprogramming of time-space information in the IED. The macroscopic shape memory behavior provides the capability to reprogram the shape of the IED, resulting in wearable and detachable functionality.

3.4. Self-Learning

Machine learning (ML) is a branch of artificial intelligence (AI) that identifies patterns in large amounts of data. It has been shown to be a valuable method in a variety of research domains during the last few decades. ML approaches have been used to discover new materials and investigate material qualities such as elasticity, plasticity, fatigue life, wear resistance, and bending. AI-empowered material science has the potential to bring about a paradigm shift in the field of material science (**Figure 7a**).[31] A fresh approach to developing layered materials using machine learning was put out by Gu et al. With this method, training is done using a database of millions of structures gleaned via finite element analysis. Additionally, they used self-learning algorithms to find high-performance materials, progressively getting rid of subpar designs to find great candidate materials (Figure 7b).[32] The findings show that their method can create microstructural patterns to produce materials that are harder and stronger. These findings were supported by testing and additive manufacturing. This new paradigm of intelligent additive manufacturing can help in the development and manufacture of novel material designs since it has computational efficiency several orders of magnitude higher than existing procedures. A new shape memory alloy was found by Texas A&M University researchers using the artificial intelligence material selection framework (AIMS) (Figure 7c).[33] The AIMS framework led to the discovery of a shape memory alloy, which has proven to be the most effective nickel-titanium-based material to date. Their data-driven structure also serves as a proof-of-concept for upcoming material advancement. The tightest hysteresis ever recorded was predicted and achieved by the shape memory alloy discovered in the AIMS-based research. To cut down on the time and resources needed for SMP development, a deep learning (DL) model was created to forecast certain SMP behaviors, including temperature changes, strain curves, response times, and stress variations.[34] By forecasting the strain curve, one may ascertain the shape memory behavior of SMP.

To build a 4D printing strategy for soft pneumatic actuator robots (SPA), Zolfagharian et al. combined nonlinear machine learning (ML) with finite element modeling (FEM).[35] To obtain the appropriate bending for particular jobs, the model seeks to forecast the geometric requirements for 4D-printed soft pneumatic actuators (SPA). The ML model successfully predicts FEM and experimental data, and it demonstrates that printing soft robots and dynamic structures in four dimensions is a practical option (**Figure 8a**). The knowledge gained from this work will help in the construction of geometric soft robots for nonlinear 4D printing issues. The thermomechanical constitutive modeling is crucial for SMP used in engineering structures and devices. However, the conventional approaches to derive constitutive models are both challenging and time-consuming, heavily relying on iterative experiments. Employing deep learning (DL) to predict the thermo-mechanical behavior of SMP under thermal cycling is a promising alternative.[36] In recent years, machine learning (ML) has been extensively used in the discovery of functional materials. However, some difficulties severely hindered the application of ML in the field of SMP and there is currently a lack of research on ML-assisted discovery of SMPs. Specific polymers can be described by "fingerprints" which characterize molecular structures in a way that computers can understand. Li et al. used the molecular dynamics code LAMMPS to simulate the thermal cycling of nine epoxy resins and curing agents. Following that, we conducted a statistical analysis to determine which fingerprints had the strongest link with each shape memory feature, particularly recovery stress and shape recovery ratio (Figure 8b).[37] This study establishes a robust basis for the selection and comprehension of atomic fingerprints, enabling the discovery of new SMPs through machine learning. Subsequently, a series of methods were proposed to tackle these challenges, specifically employing the recently introduced linear symbol in fingerprint recognition (Figure 8c).[38] A new ML framework was developed by supplementing existing datasets through reasonable approximations to predict the recovery stress of TSMPs. This framework was validated by synthesizing and testing two novel epoxy resin networks predicted by the ML models.

4. Multiscale Structure of SMPC

SMPCs can form different multiscale structures with different reinforcement phases and preparation processes, such as 0D spot structure (particles), 1D line structure (whiskers, chopped fibers, etc.) 2D plane structure (continuous fibers, electrospinning), 3D/4D body structure (3D/4D printing, foam, etc.). The design and control of SMPC's multiscale structure provide this type of material with diverse functions and properties, making it highly applicable in various fields. In-depth research on multiscale structures allows for continuous improvement in the design and processing technology of SMP materials, which in turn promotes innovative development in related fields. This advancement also brings about new opportunities and challenges.

4.1. 0D Spot Structure

SMPs can integrate different kinds of particles to change their performance and functionality to meet the demands of diverse applications. In general, functional particles can be added to polymer materials to provide them with particular functions including conductivity, magnetism, fluorescence, and photothermal

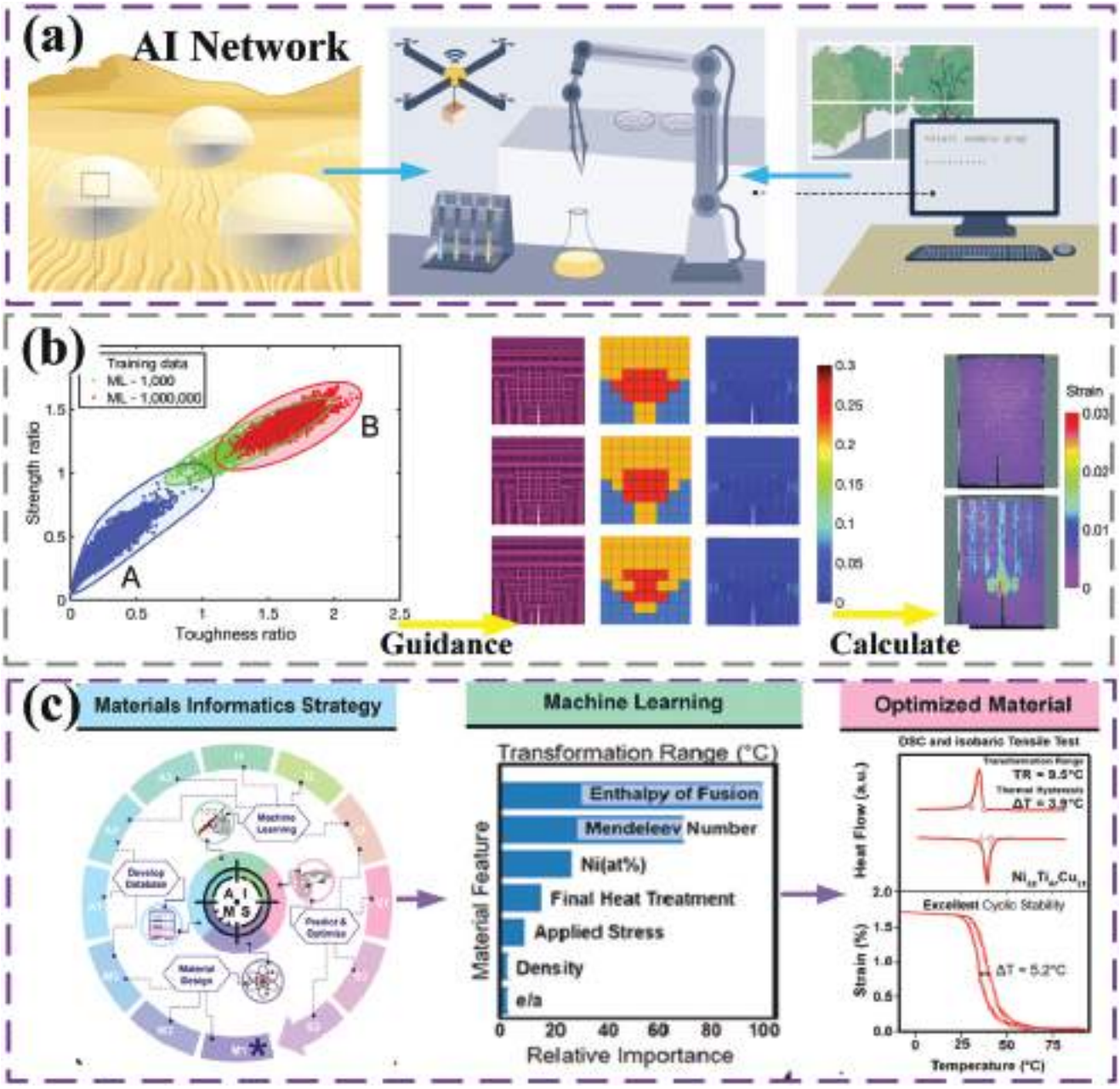

Figure 7. a) Future outlook: autonomous labs connected in an AI network. Reproduced with permission.[31] Copyright 2023, Nature. b) According to the ML's design for optimal toughness, the performance of the best 3D-printed design determined by the ML model is evaluated based on the stress-strain curve obtained from tensile experiments. Reproduced with permission.[32] Copyright 2018, Royal Society of Chemistry. c) The AIMS framework that captures the iterative workflow necessary for data-driven discovery in materials science. Reproduced with permission.[33] Copyright 2022, Elsevier.

characteristics. To improve the mechanical and thermal properties of SMP materials, it is also possible to insert nanoscale particles such as nanopowders, nanoparticles, nanotubes, etc.[39] The strong production and aggregation of nanoparticles in the resin matrix will increase the material's internal interface area, which will have an impact on the material's mechanical characteristics and interface effects. The material will experience a reduction in strength and toughness due to microcracks created by the aggregation of nanoparticles. Due to the size effect and high specific surface area of nanoparticles, they can provide a higher reinforcement effect. The mechanical, thermal, and electrical properties of polymers can all be considerably enhanced by the inclusion of nanoparticles. In contrast, the reinforcement effect of microparticles is relatively low.

Ze et al. described a new magnetic SMPC made up of two different types of magnetic particles embedded in an amorphous SMP matrix. This material system was able to execute multiple shape modifications within a single material by leveraging the magnetic properties of the particles (**Figure 9**a).[40] By

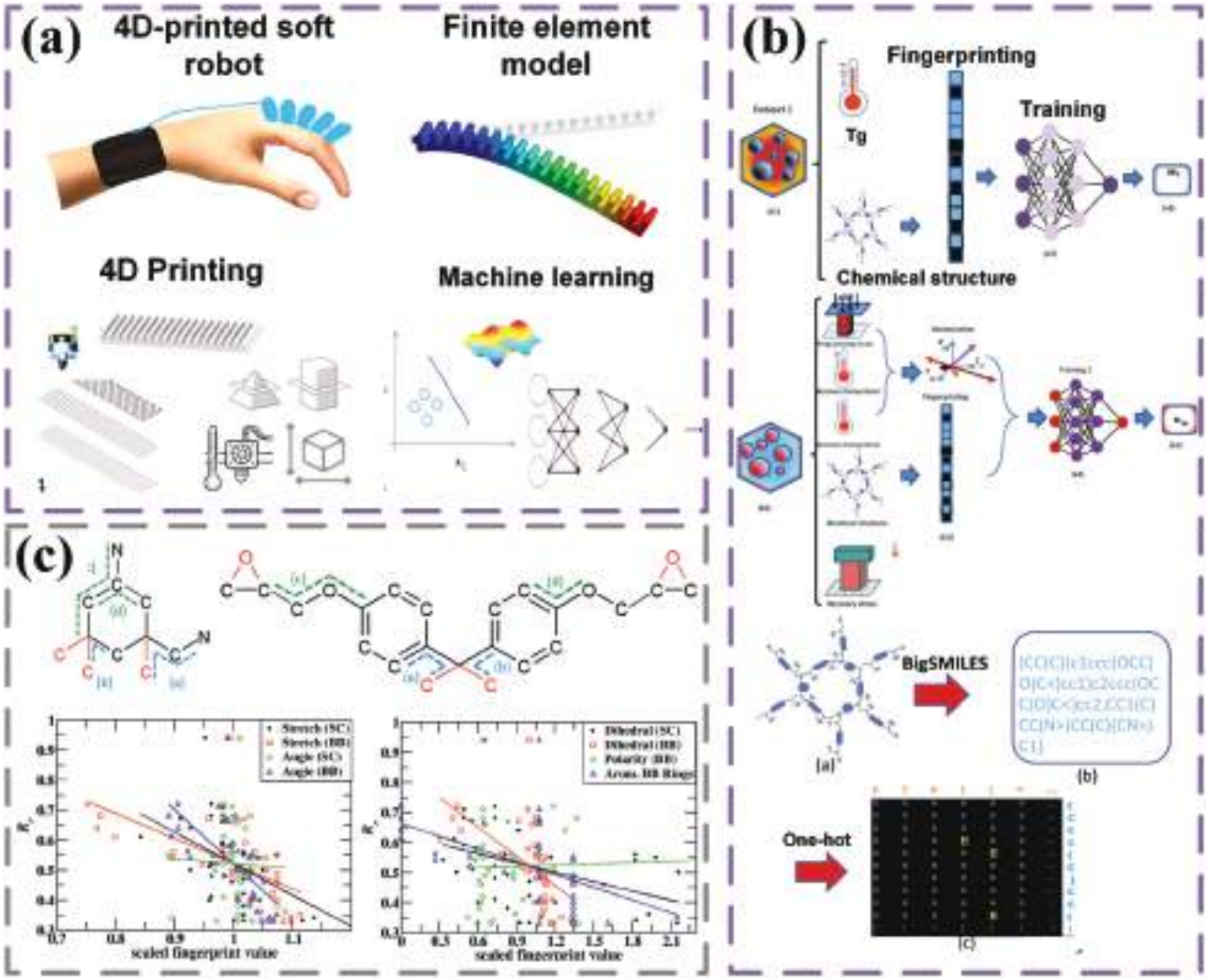

Figure 8. a) 4D printing of soft pneumatic actuator robots was conducted using nonlinear ML and FEM. Reproduced with permission.[35] Copyright 2021, Elsevier. b) Plot of the shape recovery ratio to selected fingerprint values. All fingerprints are scaled for their mean values. Reproduced with permission.[37] Copyright 2022, Elsevier. c) Pipeline for new TSMPs design. Reproduced with permission.[38] Copyright 2021, Elsevier.

softening low coercivity particles by magnetic induction heating, high remanent magnetic particles with programmable magnetization curves create rapid and reversible shape changes in an actuating magnetic field. Belmonte et al. used cholesteric liquid crystal micron-sized polymer particles as shape memory photonic pigments dispersed in shape memory adhesives, as shown in Figure 9b.[41] A multicolor coating that selectively reflects left-handed or right-handed polarized light to form any polarization-related multi-color and terrain brush pattern, in addition to a battery-free optical sensor, responsive decorating, and smart adhesive. Guo et al. developed photoinduced shape memory microparticles by enclosing a poly (D,L-lactic acid) (PDLLA) matrix in gold nanoparticles (Au@PDLLA mixed microparticles) (Figure 9c) .[42] The shape memory function system can be activated at hyperthermic temperatures and can return its suitable shape within a restricted temperature range above body temperature by activating the shape memory effect, restoring its spherical shape. The electrical resistance, however, noticeably decreases when these Ni particles are arranged in chains. Although this method was demonstrated using SMP, it can also be used with other conductive polymers. A multipurpose film with visible transparency and shape manipulation has been created by Liu et al. (Figure 9d).[43]

Doped non-close-packed (NCP) nanoparticles and a thermally responsive SMP make up the film. The internal gaps between the NPs and the polymer, which scatter light, induce reversible transparency modulation with shape deformation in the film. Using a solvent evaporation technique with CoNC@GN/P, Liu et al. created a lightweight, flexible, and malleable smart adjustable microwave absorbent material (MAM) (Figure 9e).[44] Electromagnetic waves may be absorbed at a range of angles thanks to the material's electrically driven shape memory effect, which optimizes their absorption. This shape-recovery-based MAM will have broader applications in wearable technology, chip protection, robotics, and military applications in dry, cold environments such as deserts, rain forests, or space. Bhuyan et al. employed

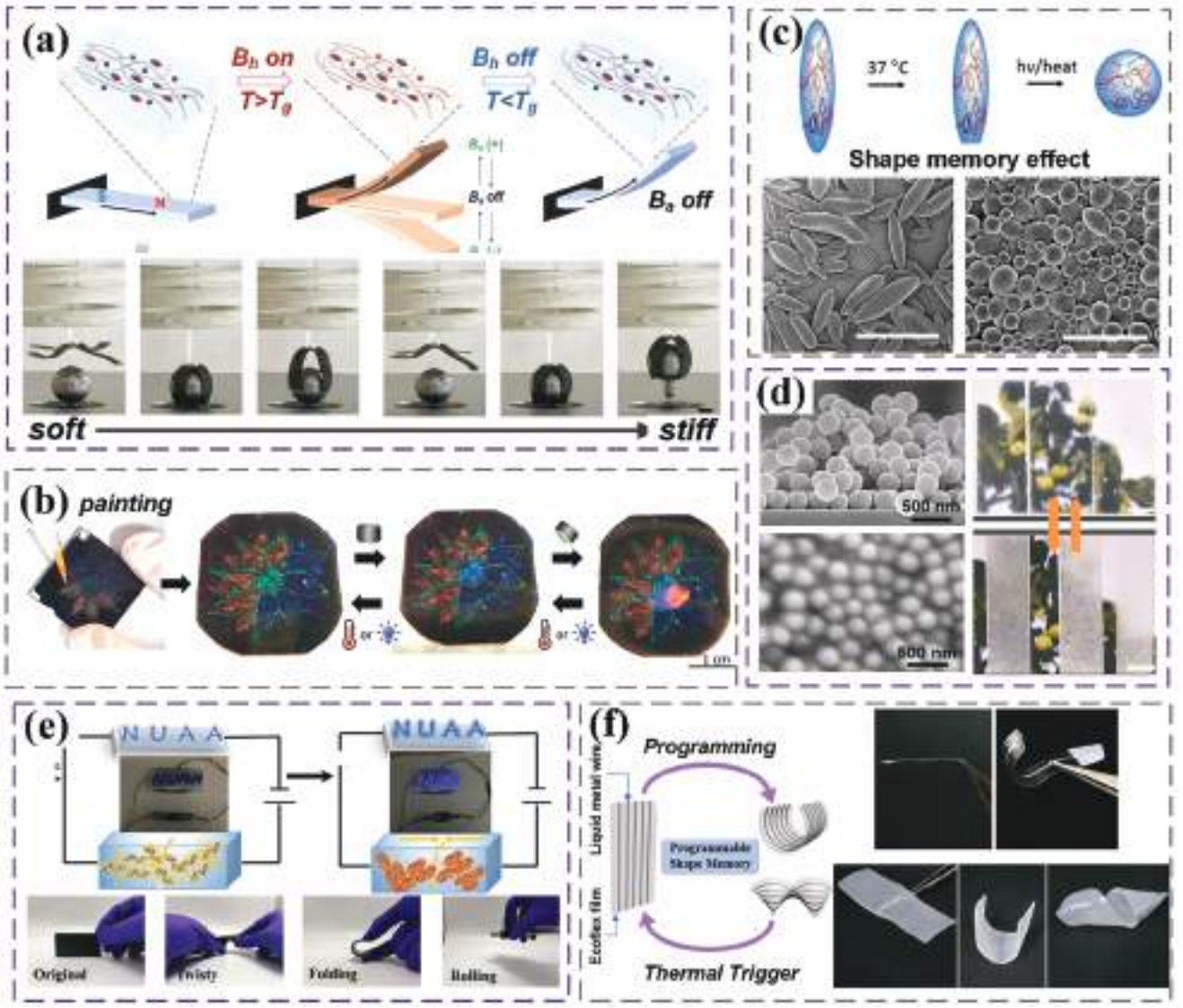

Figure 9. a) Embedded with NdFeB and Fe_3O_4 particles magnetic SMP. Reproduced with permission.[40] Copyright 2020, Wiley-VCH. b) Triple shape-memory in a brush-painted multicolor image of a flower. Reproduced with permission.[41] Copyright 2020, Wiley-VCH. c) Polymeric particle entropy-driven shape-memory effect;[42] d) SEM image of the surface of the SiO_2/EVA composite films. Reproduced with permission.[43] Copyright 2018, Royal Society of Chemistry. e) Demonstration of the self-healing phenomenon for the composite conductor in series with LEDs;[44] f) Polymer thin films embedded with liquid gallium. Reproduced with permission.[45] Copyright 2021, American Chemical Society.

gallium, a metal with a low melting point (29.8 °C), to create elastic materials with metallic conductivity and shape memory. Temperature healing can be used to regain the conductivity.[45] Stretchable electronic gadgets and soft robotics can use the conductive shape memory film with self-healing conductivity, as shown in Figure 9f.

4.2. 1D Line structure

Among the many benefits of 1D line reinforced composites are increased toughness, bending strength, wear resistance, hardness, and low weight. Applications of many kinds of 1D-line composites show unique properties. Materials can be successfully made harder and more resistant to wear by using whisker-reinforced composite materials. In addition to being simple to work with and form, short-cut fiber-reinforced composites have good bending strength and toughness. It can attain extremely high strength and lightweight design with single fiber reinforced auxiliary materials. 1D-line composites have a wide range of potential applications, great material performance, and adaptability to various technical demands.

4.2.1. Whisker Reinforced SMPC

To create electrically driven SMPCs, Liu et al. used shape memory polyurethane (SMPU) and conductively doped tin

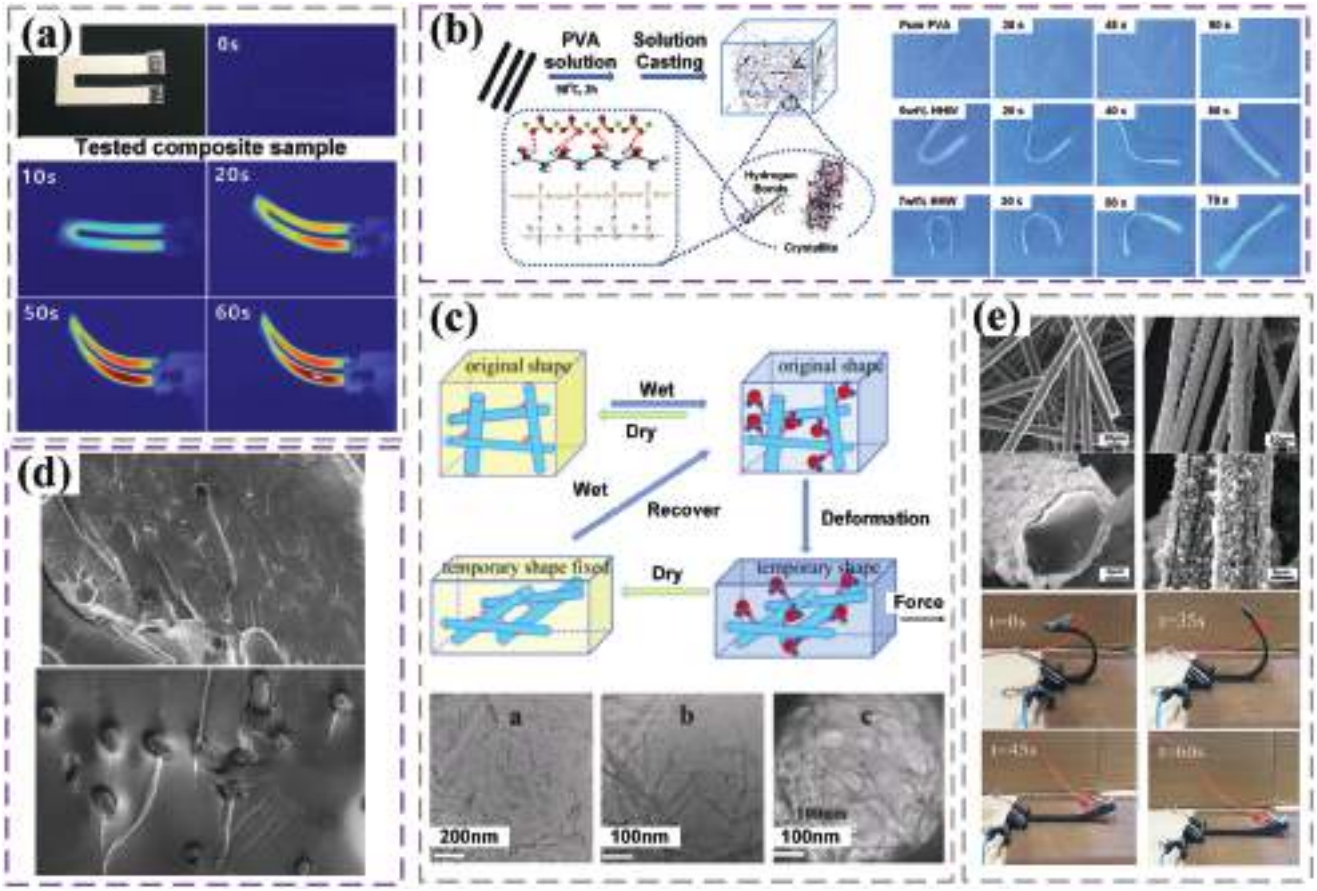

Figure 10. a) Electrically driven shape memory composite materials. Reproduced with permission.[46] Copyright 2018, Elsevier. b) Calcium sulfate hemihydrate whisker reinforced polyvinyl alcohol SMP. Reproduced with permission.[47] Copyright 2016, Royal Society of Chemistry. c) TEM images of cellulose nano-whiskers dispersed on a carbon film from the DMF suspension. Reproduced with permission.[48] Copyright 2018, Royal Society of Chemistry. d) Stress–strain curves of prepared chopped carbon fiber/epoxy composites. Reproduced with permission.[49] Copyright 2017, Elsevier. e) Shape memory of the Ag/CCF/H-EP composite activated by electricity under 60 V. Reproduced with permission.[51] Copyright 2020, Frontiers.

oxide/titanium dioxide (ATO/TiO_2) whiskers composite. The joule's heating voltage initiated the heating, and the conductive network formed by the whiskers' overlap increased the heating efficiency. Considering **Figure 10a**, The composites performed well in terms of quick heat transfer and uniform resistance, but their recovery rates in the third cycle were still higher than 2% and 96%, respectively, for the composites with 250 wt% and 2 wt% whiskers.[46] Zhao et al. created a unique SMP and added hemihydrate calcium sulfate whiskers (HHW) to polyvinyl alcohol (PVA) to improve it. The composite material's tensile strength improved by 57%, and its storage modulus reached 22.24 GPa, as shown in Figure 10b.[47] The quick switching shape memory effect (SME) that was created by the reversible production and fracture of cellulose nanowhiskers (CNW) was water-activated and entered the network in the elastic thermoplastic polyurethane (TPU) matrix (Figure 10c).[48] This study offered a fresh and practical method for quick switchable form recovery of the material via a straightforward wetting procedure.

4.2.2. Chopped Fiber Reinforced SMPC

Trans-1,4-polyisoprene (TPI) SMPCs with various mass fractions of short-cut carbon fibers were developed by Wang et al. to examine the effects of temperature and short-cut carbon fiber mass fractions on the TPI SMPCs (Figure 10d).[49] When the mass percentage of short-cut carbon fiber was 8%, the TPI SMP demonstrated good shape memory performance and optimal mechanical characteristics. Park et al. investigated the impact of 2 mm short-cut carbon fibers on the resin interface interaction based on SMEP supplemented with short-cut carbon fiber-reinforced matrix and achieved the control of CCFs/EP shape recovery carrier by the amount of CCFs.[50] Short-cut carbon fiber (CCF) was treated by Wang et al. into silver-plated short-cut carbon fiber (Ag/CCF), which was then inserted into hydrogenated bisphenol. To create electrically induced SMPCs, use an epoxy resin (H-EP). When the concentration reached 1.8 wt%, the Ag/CCF/H-EP composite material met the criterion for thermal conductivity, electrical conductivity, and permeability (Figure 10e).[51]

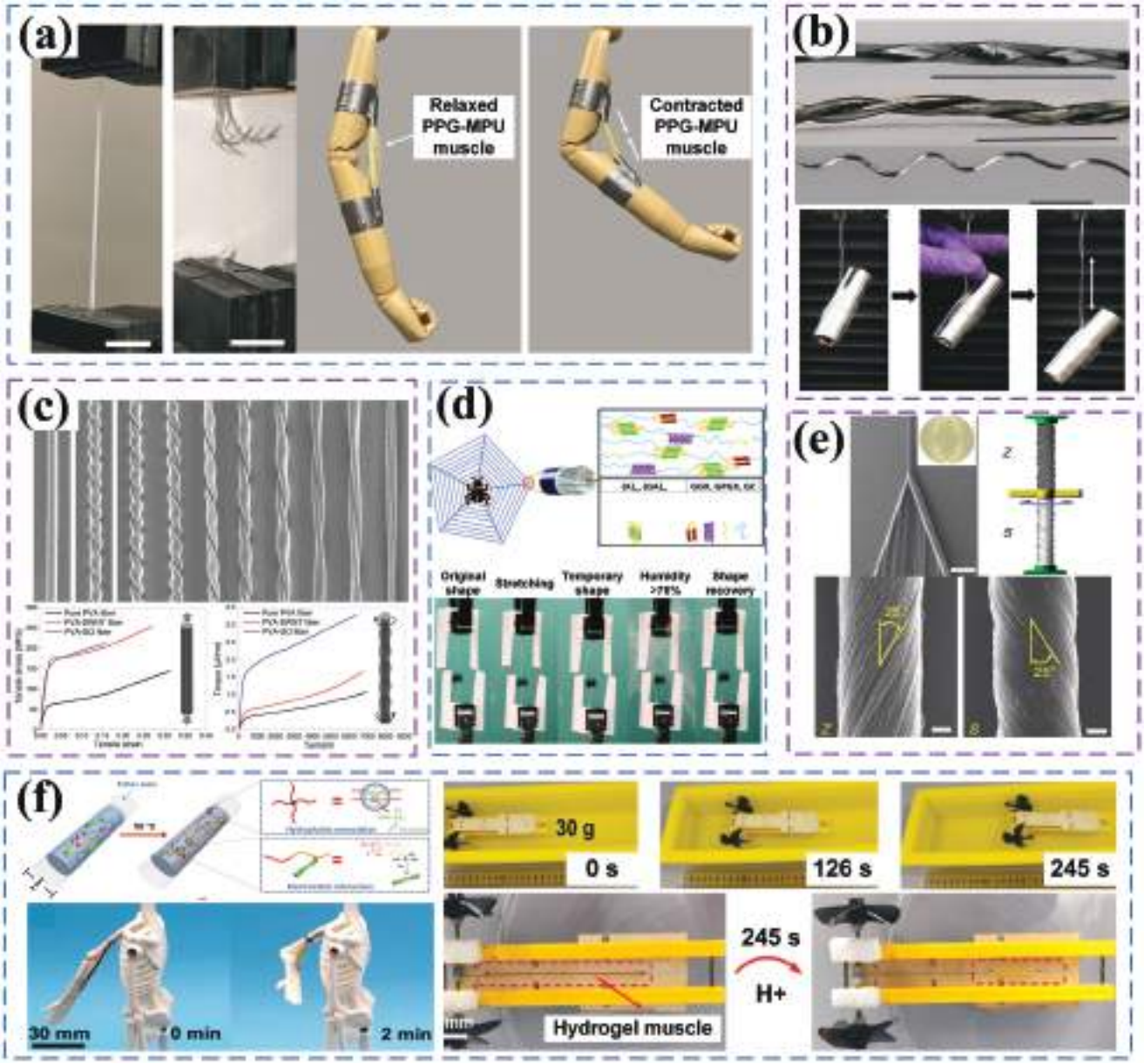

Figure 11. a) A full-size mannequin arm (0.6 kg) is actuated by a synthetic muscle made of prestrained films of PPG-MPU (3.8 g). Reproduced with permission.[52] Copyright 2021, American Chemical Society. b) SMP fibers for rotating microengines. Reproduced with permission.[53] Copyright 2019, American Association for the Advancement of Science. c) By melting the metallic core, forming the fiber, and letting the metal cool, conductive fibers with diverse geometries can be produced. Reproduced with permission.[54] Copyright 2019, Wiley-VCH. d) The fiber's recovery to its original shape after exposure to dampness is caused by a shape memory programming process. Reproduced with permission.[55] Copyright 2019,Frontiers. e) Dual Archimedean-type twist insertion during spinning captured in a SEM picture from a CNT forest. A twin Archimedean scroll is depicted in the insetReproduced with permission.[56] Copyright 2014, Nature. f) Movement of the boat model powered by 2 Macid through the hydrogel muscle. Reproduced with permission.[57] Copyright 2023, Elsevier.

4.2.3. Smart Fiber Reinforced SMPC

A strain-induced supramolecular nanostructure synthesis technique is used to produce unidirectional SMPs with high energy density.[52] Strong directional dynamic bonds are created during the straining process, creating stable supramolecular nanostructures that enfold the stretched chains, as shown in **Figure 11**a. The stretched chains shrink back to their initial disordered condition as a result of the dynamic bonds breaking when heated. Entropy energy is effectively stored via this process. A high-energy microengine based on shape memory and its nano-composite fibers was created by Yuan et al.[53] PVA and its nanocomposite materials make up the shape memory fibers, which can store mechanical energy and quickly release it by heat stimulation to enable high-energy and quick rotation, as shown in Figure 11b. The performance of biological muscles can be

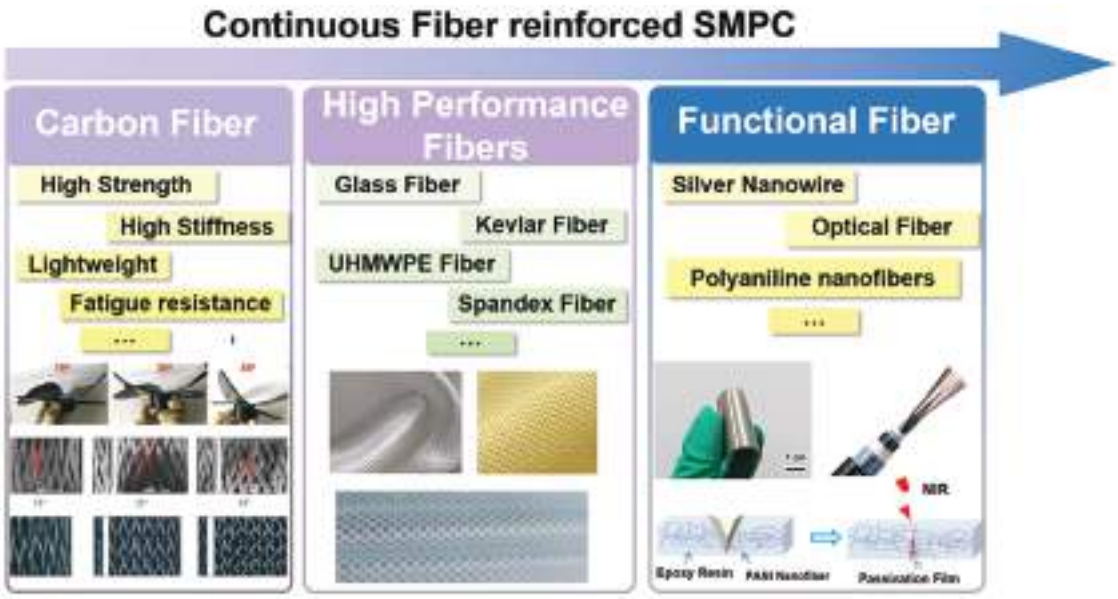

Figure 12. The evolution of SMPC reinforced with continuous fibers.

imitated using spider dragline silk, which can adapt to varying humidity levels in the surroundings. A common shape memory characteristic is the humidity-responsive supercontraction of spider silk. Through the injection of molten gallium into a hollow fiber core, Dickey et al. created an elastic fiber with shape memory properties. By melting the metal core to shape the fiber, various geometric structures of conductive fibers are obtained after the metal cools down as shown in Figure 11c.[54] The gallium core can change from solid to liquid under low heating conditions. The addition of a solidified core can boost the fiber's effective modulus from 4 to 1253 MPa, and the increased stiffness allows the fiber to preserve its deformed shape. This process permits the fabrication of shape memory fibers utilizing any hollow elastic fiber.

Major ampullate 2 (eMaSp2) fibers, which feature several polyalanine and proline motifs, were genetically altered by Hu et al. to produce this behavior for the first time.[55] Equilibrium molecular dynamics (EQMD) simulations were run to assess eMaSp2 over 200 ns to further validate this shape memory hypothesis (Figure 11d). This study provided new insights into the clever behavior displayed by synthetic spider silk by demonstrating that eMaSp2 fibers are humidity-sensitive shape-memory materials. To produce overdamped dynamic responses, a yarn object made of high-damping viscoelastic paraffin and polystyrene-poly(ethylene-butene)-polystyrene copolymer was utilized (Figure 11e).[56] With position control of actuators employing twist damping that was inspired by spiders, the application range of twisted rotating CNT muscles was considerably increased in particular. In the areas of biomedicine and bioengineering, polymer hydrogels have been found as viable possibilities for imitating natural muscles. Their use as artificial muscles has been constrained, nonetheless, by their low working capacity and low strain. The development of hydrogel-based artificial muscles with superior mechanical properties-high strain capabilities (up to 75%) and high specific work capacity-has been made possible by the incorporation of thermally controlled nanofiber composite reinforcement (Figure 11f).[57] The high-strain, high working capacity, and equivalent output efficiency of these hydrogel muscles suggest a broad range of potential uses.

4.3. 2D Plane Structure

4.3.1. Continuous Fiber Reinforced SMPC

Fiber-filled reinforced SMPCs outperform particle-filled reinforced SMPCs in terms of strength, modulus, creep resistance, and relaxation resistance, offering improved mechanical performance. Compared to pure SMPs, fiber-reinforced SMPCs exhibit much higher stiffness and strength. Additionally, the mechanical properties of the composites can be adjusted by varying the fiber volume fraction, layering position, and layering orientation, as shown in **Figure 12**. As a result, numerous studies have been done to improve the recovery stress and recovery rate of fiber-reinforced SMPCs. However, adding fiber reinforcement inevitably lowers the SMPCs' extensibility and recovery rate. Numerous academics have conducted research projects to lessen the impact of these limitations.

Shape memory epoxy resin composites (SMEPCs) with good mechanical properties were produced by Liu et al. by incorporating various short and continuous carbon fibers (CFs) into the matrix of SMEP.[58] With a maximum recovery force of 4.4 GPa at room temperature and a storage modulus of up to 37 GPa, the developed SMEPC demonstrated strong shape memory capabilities. These features exceeded those of the average SMP systems currently on the market by at least one order of magnitude. A research finding on SMPC with a spatially deployable structure was given by Ken et al.[59] The thermosetting styrene used in the composite material served as the matrix, while the reinforcement

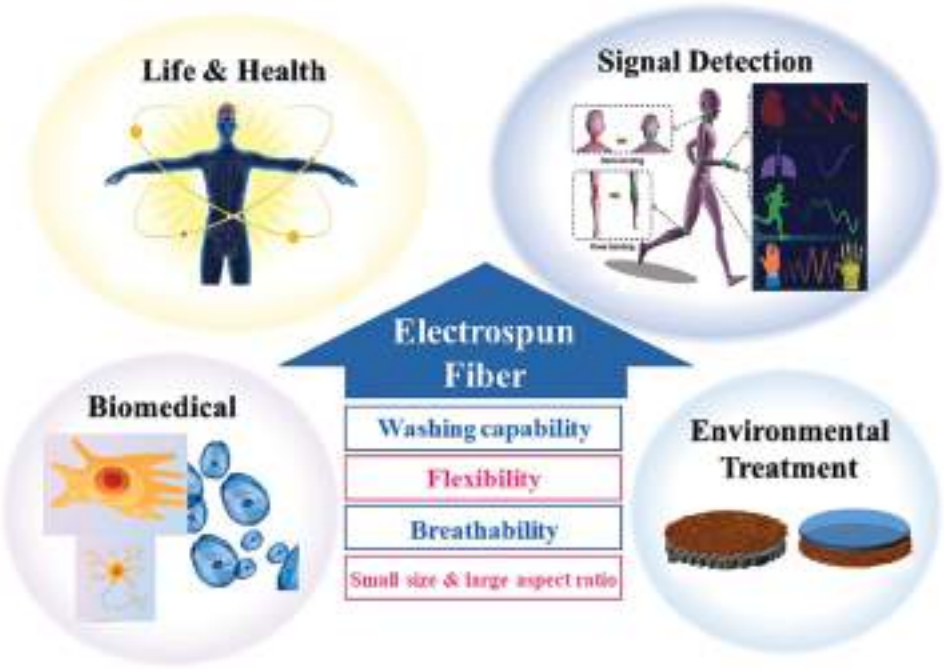

Figure 13. Overview of SMP electrospinning.

textiles used were satin and plain weave. Preimpregnated materials were layered and compressed to create the SMPC. The melting point of thermosetting styrene was roughly 95 °C. The study also looked into how radiation under certain circumstances could enhance polymer materials' capacity to resist deformation due to heat. As reinforcements for SMP, in addition to carbon fibers, glass fibers, aramid fibers, and other functional fibers have also been employed, making them essential components for the creation of SMPCs. Glass fiber reinforcement was added to SMPCs by Ali et al.[60] The results of the study show that the mechanical characteristics of the material are greatly improved by the addition of glass fiber content. Additionally, adding coupling agents enhances the link between the fiber and matrix, considerably enhancing the composite material's strength. Silver nanowires (AgNW) and PI were mixed by Yao et al. to create thin film electrodes with high conductivity and stability.[61] AgNW simultaneously demonstrates conductivity and infrared absorption, enabling the flexible electrode to regain its original shape under Joule heating, electrical stimulation, and light stimulation. This work enhances the potential applications and value of flexible electrodes by integrating electrically and optically driven shape recovery methods. Such stable electrodes may find use in electrical devices including batteries, screens, and mobile phones.

Applications in large-scale sectors like aviation and aerospace hold considerable promise for long fiber-reinforced SMPCs. Although long fiber-reinforced SMPCs have greatly increased in strength and modulus when compared to pure polymers, the material's recovery force has only been marginally enhanced. The healing rate of the material may also be lowered as a result of the fibers. For the application of SMPs in the field of actuation, however, enough recovery force and rate are essential. The successful application of SMPCs in aviation and aerospace engineering therefore requires overcoming these difficulties.

4.3.2. Electrospinning SMPs

Electrospinning is a method used to manufacture polymer fibers with sizes ranging from nanometers to micrometers and has been widely used to manufacture fibers with diameters ranging from 50 to 500 nm.[62] Electrospun processing can be used to process a variety of polymer materials, including PU, PLA, PCL, and epoxy ethane. Wide-ranging applications for these electrospun fibers include scaffolds for tissue engineering, antimicrobial products, drug delivery systems, membrane materials, filters, membrane materials, reinforced fibers in composite materials, soldier protective clothing, optical and electronic applications, and drug delivery.[63] Various types of fiber structures have emerged with the innovation of spinning technology. Shape memory micro/nanofibers have been successfully applied to prepare nonwoven, core-shell, hollow, bead, and directional structures, as shown in **Figure 13**.[64]

Zhang et al. successfully created core–shell shape memory polymer fibers (SMPF) with epoxy resin core and PCL shell through UV crosslinking. At a temperature of 70 °C, the reaction speed of the fibers is faster, and the entire shape memory recovery process only takes 6.2 s.[65] Moreover, they created composite nanofibers by combining Fe_3O_4 nanoparticles with Nafion. PU molecules were aligned along the fiber axis during the electrospinning process, producing directionally structured electrospun nanofibers, as illustrated in **Figure 14a**.[66] With a wide range of transition temperatures between 55 °C and 170 °C, Zhang et al.'s electrospun Nafion ultrafine fiber membrane demonstrated numerous SMEs and returned to its original shape at the right deformation temperatures.[67] Wei et al. suggested a method, seen in Figure 14b, for producing conductive polymer fiber composites that are incredibly thin, flexible, and possess strong shape memory and electromagnetic

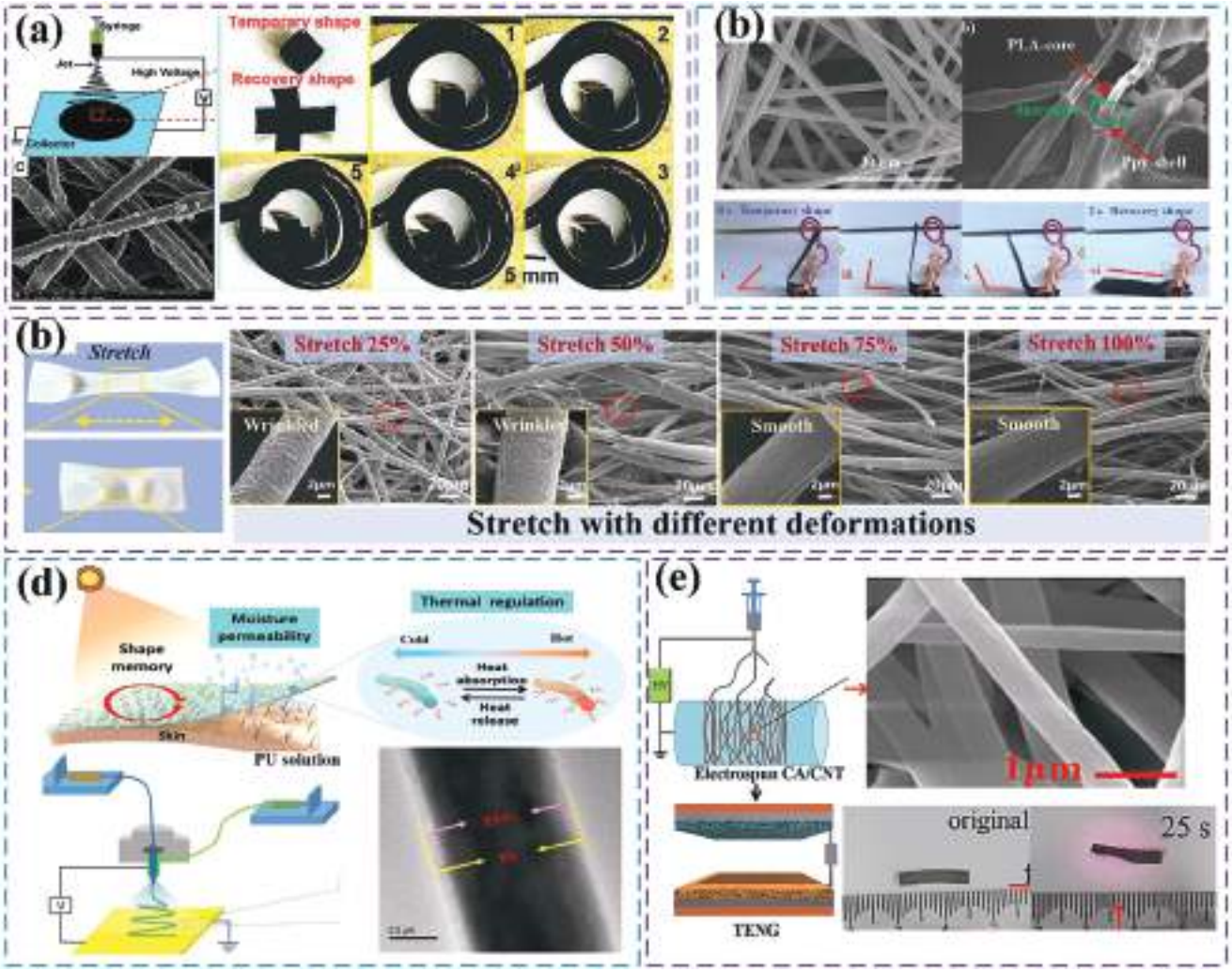

Figure 14. a) Nafion/Fe_3O_4 composite fibers before and after magnetic field driving. Reproduced with permission.[66] Copyright 2022, Elsevier. b) Electric-driven stretching SME. Reproduced with permission.[68] Copyright 2022, Elsevier. c) The scar effect of electrospun fiber membrane with folded fibers. Reproduced with permission.[69] Copyright 2023, Wiley-VCH. d) Membranes with shape memory and coaxial electrospinning that can store thermal energy. Reproduced with permission.[70] Copyright 2021, Elsevier. e) Electrospinning cellulose acetate (CA)/carbon nanotube nanofiber composite material. Reproduced with permission.[71] Copyright 2023, Elsevier.

interference shielding qualities.[68] Highly crosslinked ethylene vinyl acetate copolymer (EVA) fiber membranes were achieved by electrospinning and UV crosslinking, providing new opportunities for electromagnetic shielding membranes and intelligent manufacturing (Figure 14c).[69] These controllably formed fiber membranes were used to study the intelligent controlled release of doxorubicin. The drug release rate of the stretched fiber membrane is higher than that of the unstretched fiber membrane because of the unfolding of wrinkles. When it comes to the flow of heat between the human body and its surroundings, intelligent fabrics are essential (Figure 14d).[70] Phase-change fiber membranes with aligned fibers and a "core-shell" structure fabricated by coaxial electrospinning technology demonstrate good shape memory performance under temperature stress. This gives the membrane adjustable breathability by enabling its macroscopic shape and microporous structure to adapt in response to temperature variations spontaneously. To explore the application of nanofiber materials in sensors, cellulose nanofiber composites based on acetic acid were created by the electrospinning process (Figure 14e).[71] The study shows that the nanofiber composite material can draw a load 1050 times its weight when employed in photothermal actuators, and it has a wide range of potential applications in optically sensitive driving devices. This greatly expands the material's potential applications in numerous industries.

4.4. 3D/4D Body Structure

4.4.1. 3D/4D Print SMP

Metamaterials are functional materials that have been purposefully created and have amazing physical qualities that go above and beyond those of natural materials. They may have periodic or nonperiodic structure arrays. Innovative mechan-

Figure 15. Schematic diagram of 4D printing overview.

ical functional features like complex multistability, variable stiffness, and negative Poisson's ratio are made possible by mechanical metamaterials through the logical optimization of structural design. The capacity to program metamaterial structures and properties is made possible by the union of smart materials with programmable attributes, as shown in **Figure 15**.

Through the use of SMP with shape-memory qualities, it is also possible to create mechanical metamaterials with a negative Poisson's ratio that are structurally and mechanically tunable. The stretching of chiral mechanical metamaterials based on the DLP method was proven by Xin et al. (**Figure 16a**).[72] They were able to give the metamaterials customizable and programable mechanical properties as well as Poisson's ratio behavior by combining the shape-memory capabilities of printing materials. To produce a torsional mechanical metamaterial with nonlinear biomimetic mechanical performance, they also developed a mechanical pixel array, helical microstructure, and 4D printing techniques. The combination of 4D printing proved the tunability, programmability, and reconstructions of the mechanical behavior of the metamaterials due to the significant reliance of mechanical properties on geometric parameters. By incorporating bending ribbons with multi-level microstructures into metamaterials and combining this with 4D printing technology, Li et al. were motivated by the idea of fractal geometry and were able to create stretchable mechanical metamaterials with adjustable, programmable, and reconfigurable mechanical properties, such as nonlinear stress-strain behavior and Poisson's ratio (Figure 16b).[73] Using high-precision additive manufacturing technology (stereolithography) for 4D printing, Yang et al. created lightweight metamaterials with geometric reconfigurability, variable functionality, and mechanically adjustable characteristics.[74] As a result, the metamaterial's stiffness, geometrical make-up, and functioning can be changed reversibly, adjusting to a variety of unpredictably occurring situations such as shifting external stresses and complicated settings (Figure 16c). Additionally, Li et al. created a thermally stimulated 4D printed tunable local resonant elastic metamaterial, evaluating its adaptive bandgap switching, and using it to create programmable and tunable elastic wave transmission channels (Figure 16d).[75] This study expands the uses of 3D-printed thermoplastic SMPs by providing new prospects for the design and manufacture of smart devices for elastic-wave control and vibration isolation.

Lv et al. used 3D printing, self-folding assembly, and ceramics made from elastomers to create a silicone rubber-based nanocomposite material that is simple to print, deform into intricate elastic shapes, and then turn into mechanically durable ceramics (**Figure 17a**).[76] 4D printing technology was used to create iconic porcelain origami constructions with intricate curves, like the butterfly, Sydney Opera House, rose, and garment. Origami-inspired mechanical metamaterials with a variety of topological parameters were created by Zhao et al. and demonstrated exceptional mechanical qualities, as shown in Figure 17b.[77] To track gait, achieve self-powering and self-sensing, and build friction-electrified nanogenerators (MS-TENG) based on metamaterial structures. By using 4D-printed microstructures in place of conventional high aspect-ratio structures, Gu et al. reported a novel capillary-force-induced self-assembly technique, enabling bidirectional (conventional self-assembly and 4D self-assembly) and reversible self-assembly, as shown in Figure 17c.[78] The crosslinking density within the photoresist microstructures can be distributed asymmetrically by adjusting the distance between the dual-photon scanning channels. The printed structures can be made flexible and vertical thanks to the asymmetric crosslinking density.

For independent continuous fiber-reinforced composite 3D printing, Wong et al. suggested a 4D printing technique based on direct ink writing, as shown in **Figure 18a**. The liquid crystal elastomer composite's imbedded continuous fibers are crucial for improving mechanical characteristics and permitting bending deformations. The ability of continuous fibers to sustain different structures during printing improves the mechanical performance and deformation capacity of 4D printed structures. Zeng et al. developed a dual-feed-channel 3D printer based on fused deposition modeling (FDM) for the manufacture of continuous carbon fiber-reinforced shape memory polylactic acid-based composites (CFRSMPC).[79] The electrically induced shape memory effect of 4D printed CFRSMPC was explored by using electrical heating during form recovery investigations (Figure 18b). The specimens' form recovery rate was greater than 95%, demonstrating the durability and viability of the resistance heating technique. In additional research, the quantitative

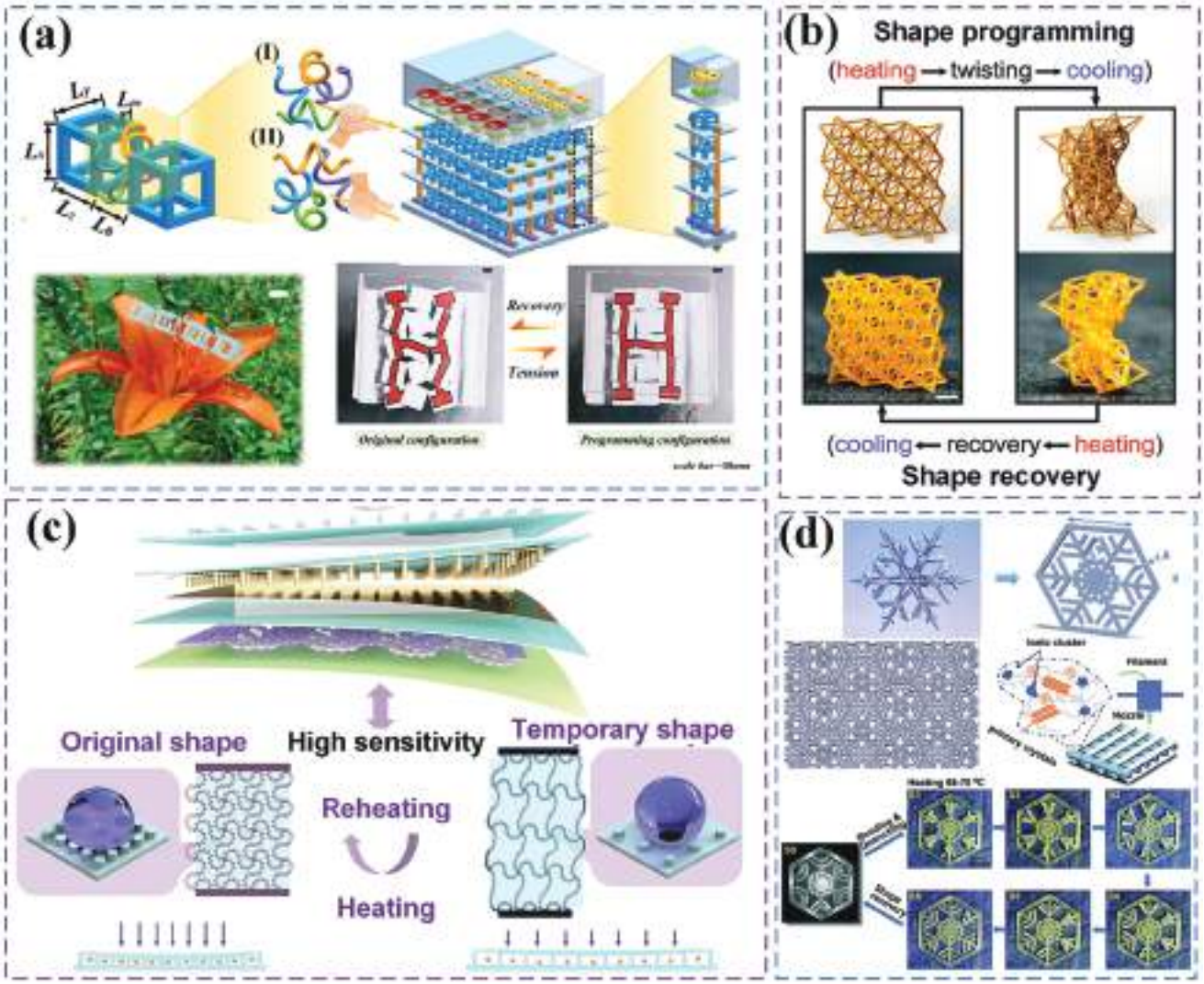

Figure 16. a) Tensile torsional coupling mechanical metamaterials printed in four dimensions. Reproduced with permission.[72] Copyright 2022, Wiley-VCH. b) A multilayer flexible form memory sensor's construction and shape memory cycle are shown schematically. Reproduced with permission.[73] Copyright 2023, Elsevier. c) Stereolithography printing of lightweight metamaterialsReproduced with permission.[74] Copyright 2019, Royal Society of Chemistry. d) Crystal cells like snowflakes make up tunable elastic metamaterials. Reproduced with permission.[75] Copyright 2021, Elsevier.

impact of temperature and bending angle on the resistance of the CFRSMPC throughout the programming and recovery processes was examined.[80] Lightweight honeycomb composites are employed in energy absorbers, truss structures, laminates, and other applications as low-density high-performance structural materials. A lightweight honeycomb structure based on triangular infill was created by Dong et al. after path design, G-code generation, and sample printing (Figure 18c).[81] To create new 4D-printed honeycomb structures based on triangular infill, continuous Kevlar strands were added to PLA filaments. The researchers created a gel-like ink that can be 4D printed in one step at room temperature using regular 3D printing nozzles (Figure 18d).[82] An oscillating suspension of Cu, EGaIn (eutectic gallium-indium liquid metal), and water makes up the majority of the ink. A flat metal construction that gradually assumes the shape of a spider was printed to show off this effect.

4.4.2. Shape Memory Foams

Shape memory polymer foam (SMPF) is a novel form of smart polymer structure with holes constructed from SMPs. The advantages of conventional foam's light weight and excellent compression ratio are combined with SMPs' distinctive shape memory effect to create SMPF. Initially, SMPFs were made using conventional chemical foaming and physical foaming techniques. However, as SMPF research has developed, many shaping techniques for SMPF have been found. These procedures include microwave foaming, phase separation foaming, composite foaming, particle leaching, and supercritical carbon dioxide foaming.[83] Recently, the immersion method in addition to gas foaming and particle leaching was used to create SMPU foam.[84,85]

3D graphene foam (GrF) has shown promise as a practical reinforcing material for SMP epoxy composites. Idowu et al.

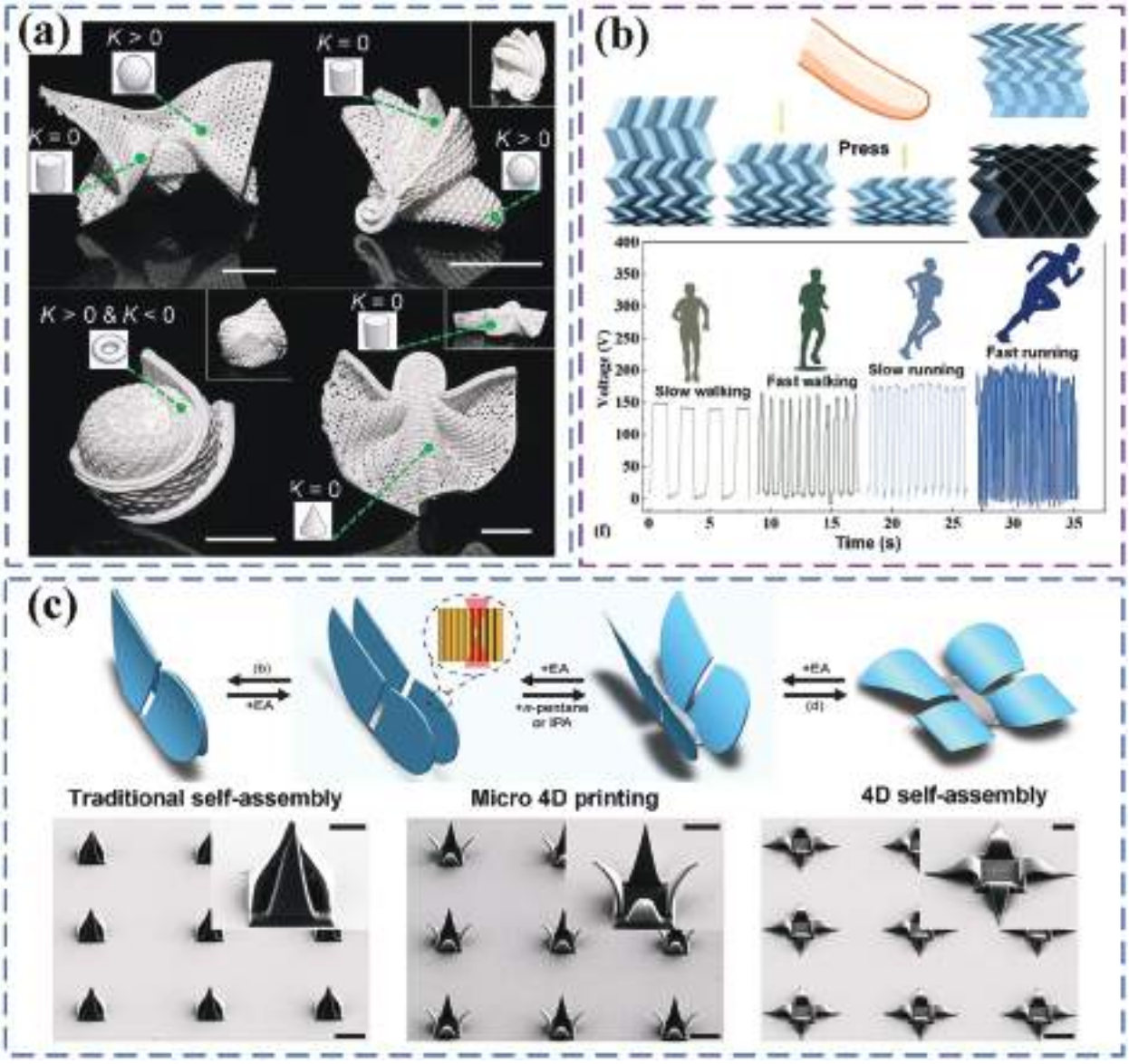

Figure 17. a) 4D printing of complex ceramic origami. Reproduced with permission.[76] Copyright 2018, American Association for the Advancement of Science. b) Functional application of Miura woven metamaterials with integrated frictional and piezoelectric sensing functions. Reproduced with permission.[77] Copyright 2023, Elesvier. c) Micro origami and packaging based on 4D printing microstructure self-assembly. Reproduced with permission.[78] Copyright 2021, Wiley-VCH.

found that when 0.13 wt% GrF was added to mold-injected SMP epoxy resin, the Tg increased by 19%.[86] Zhao et al. developed liquid metal SMP foam (LM-SMF) by incorporating a conductive and thermally conductive liquid metal (LM) into a pliable foam structure (**Figure 19a**).[87] The foam skeleton can be reversibly compressed based on the thermoresponsive shape memory phenomenon, allowing the transfer of LM between the connected and unconnected states. Since the LM-SMF's resistance can be constantly adjusted from 0.8 (conductive) to 200 M (insulator), and its thermal conductivity may vary by up to 4.71 times, it appears that it can regulate heat both electrically and thermally. They also created a smart, controlled-shape, liquid-permeable memory foam material (Figure 19b).[88] While maintaining good wettability, the foam's pore size can be changed and self-maintained in the range of 28 nm to 90 m. This property enables exact control of the permeation flux of water or oil and allows for precise control of the permeation phenomenon. Therefore, there are several potential uses for this foam material in sectors such as the exact control of small molecule release. A straightforward method of producing smart electromagnetic shielding materials based on EPA composite foam with shape memory capabilities was put out by Wang et al. (Figure 19c).[89] To create SMP foam, sacrificial templating, and chemical cross-linking techniques were used. This allowed for the modification of EMI shielding performance through self-fixing deformation without the inclusion of extra insulating polymers. For the

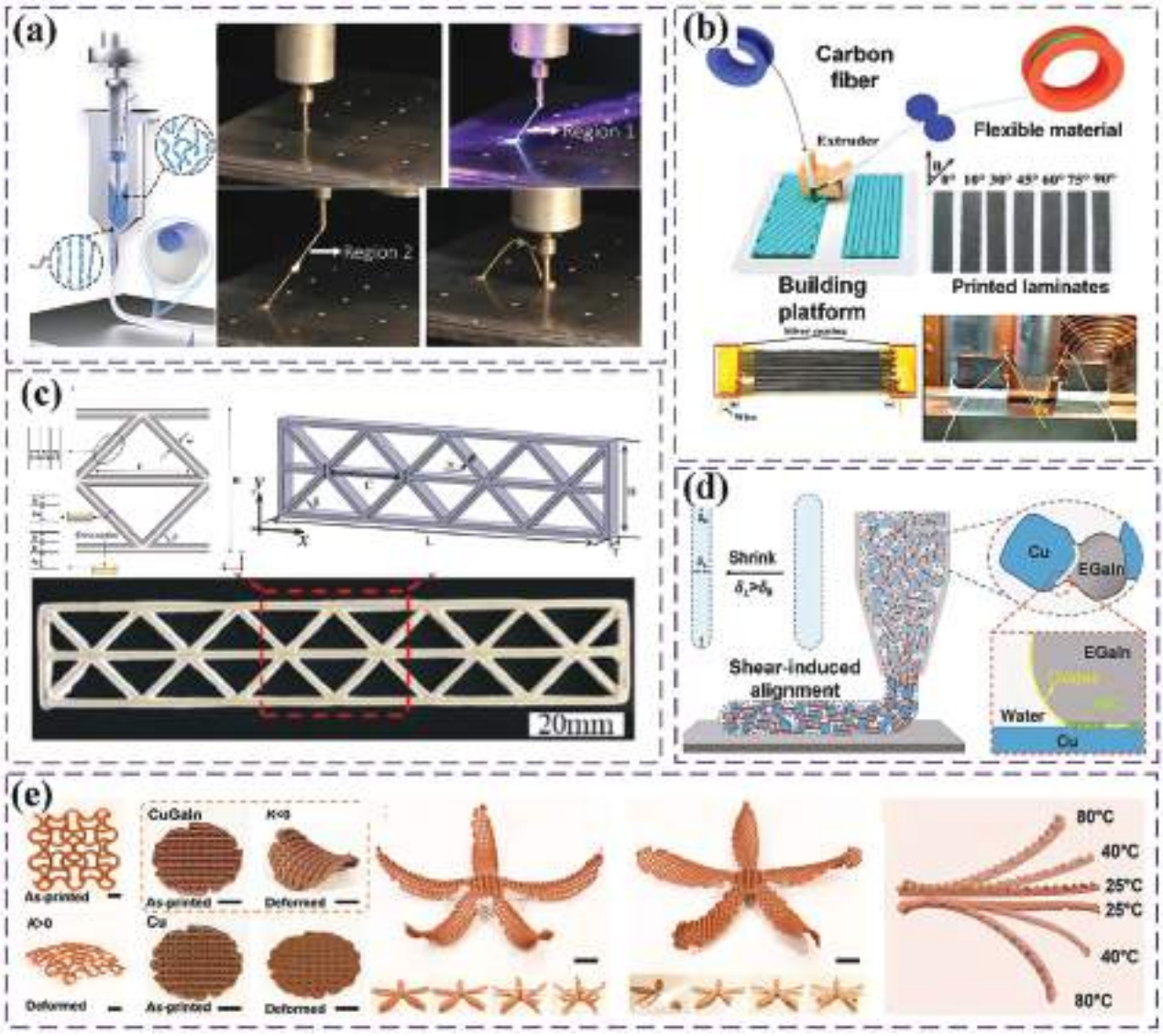

Figure 18. a) Angle truss components made of continuous fiber reinforced liquid crystal elastomer composite materials using 4D printing. Reproduced with permission. Copyright 2023, Nature. b) Improved FDM-based preparation of CFRSMPC specimens made of continuous carbon fiber. Reproduced with permission.[79] Copyright 2020, Elsevier. c) Lightweight honeycomb CFRC 4D printed with continuous fiber reinforcement. Reproduced with permission.[81] Copyright 2021, Elsevier. d,e) 4D-printed Cu-EGaIn structures with programmed curvatures. Reproduced with permission.[82] Copyright 2023, Elsevier.

creation of shape memory materials with adjustable electromagnetic shielding qualities, this finding has significant ramifications. SMPs can exhibit excellent strain-induced performance as well as the ability to modulate electrical and thermal conductivity thanks to a multiscale designed graphene foam that Zhou et al. reported has an elastic 3D network structure and a microstructure primarily made of monolayer graphene (Figure 19d).[90] Guo et al. used SMPCs based on cross-linked poly-cyclooctene as a matrix and carbon nanotubes as fillers to develop a high-performance, foldable, and salt-clogging monitoring flexible solar steam generating system (Figure 19e).[91] Excellent shape memory effects allow this interface evaporation system to fold down to 1/9 of its original size and unfurl on its while in use. This research illustrates the potential uses of SMPs in several industries, including flexible solar steam generating systems, strain-induced performance augmentation, and electromagnetic shielding.

5. Application

SMPs have uses ranging from oil extraction and sealing to drug distribution due to their considerable deformation, variable stiffness, and huge shrinkage. As a result, in the aerospace sector, its high compression ratio conserves storage space and acts as the motor for artificial muscle in intelligent bionics. It is also extensively utilized in the biomedical industry as well as other industries and has strong biocompatibility. It has become more and more popular among scholars in recent years.

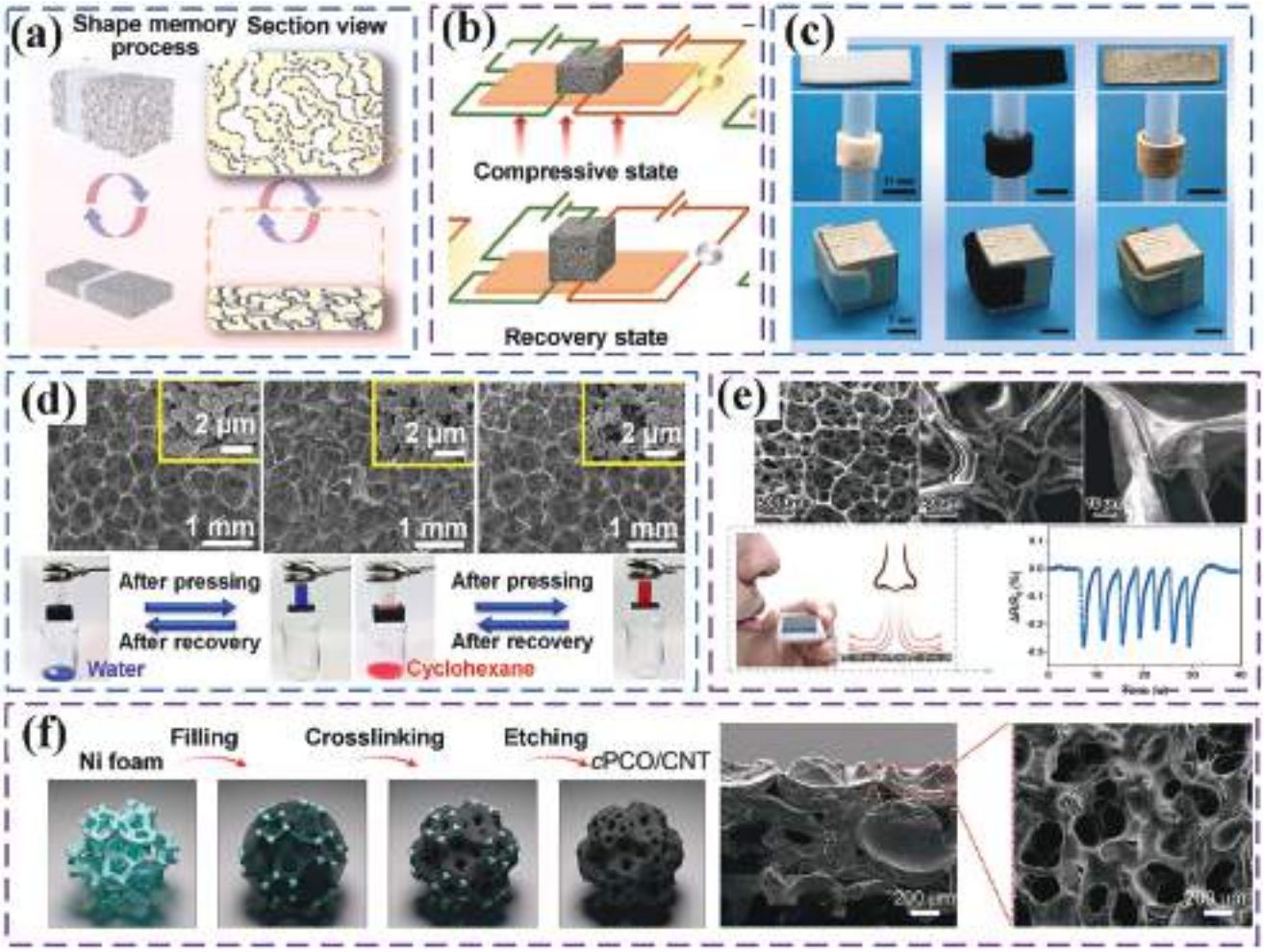

Figure 19. a) LM creating open circuit/path in foam, self-feedback integrated electric/thermal switch schematicReproduced with permission.[87] Copyright 2023, Wiley-VCH. b) Shape memory foam's structure and hydrophilic On/Off characteristicsReproduced with permission.[88] Copyright 2020, American Chemical Society. c) Foam's capacity to adapt to shape and to remember itReproduced with permission.[89] Copyright 2023, Elsevier. d) Electrically triggered shape recovery method for the SLGF-SMP composite sampleReproduced with permission.[90] Copyright 2022, Wiley-VCH. e) Solar evaporator with shape memory. Reproduced with permission.[91] Copyright 2021,American Chemical Society.

5.1. Aerospace Applications

The construction of new expandable structures now has a material basis thanks to the introduction and extensive study of SMPCs. Expandable structures made of SMPCs provide answers to several problems with conventional expandable structures, such as complexity, weight, impact resistance, instability during expansion, and limited testability.

As seen in **Figure 20**a,b, ILC Dover developed a parabolic space expansion reflector with a high compression ratio using SMEP tubes and spring steel.[92] Leng et al. developed SMEP which is thermosetting and investigated the effectiveness of the polymer and its composites in harsh space settings.[7a,b,93,94] After completing the material-level in-orbit verification of SMPC in 2016, the ground-based validation of rigid solar arrays based on SMPC hinges was completed in 2018. Additionally, in 2020, SMPC-based flexible solar arrays were validated in space,[95] as shown in Figure 20c,d. They also created a structure for SMPCs that can be folded and unfolded in the style of a papyrus scroll (Figure 20e).[96] On-Mars qualification was ultimately accomplished with China's Tianwen-1 mission, which communicated photos of the deployed five-star red flag through the Zhurong rover. It is the first validation in deep space of a self-deployable approach based on SMPCs, and more applications are anticipated to follow. As the first SMPC structure in Mars exploration engineering to be used internationally, it flew 475 million kilometers and completed the first controllable dynamic deployment of the Chinese national flag on Mars, as shown in Figure 20g,h.[96a,97]

5.2. Robotics

Soft robots that utilize SMPs can be employed for tasks such as grabbing, walking, swimming, flying, and sensing control. Recently, the actuators of SMPs with options for deterioration and self-healing have been presented for use in robotics. Their driving geometry and switch temperature can be reprogrammed through

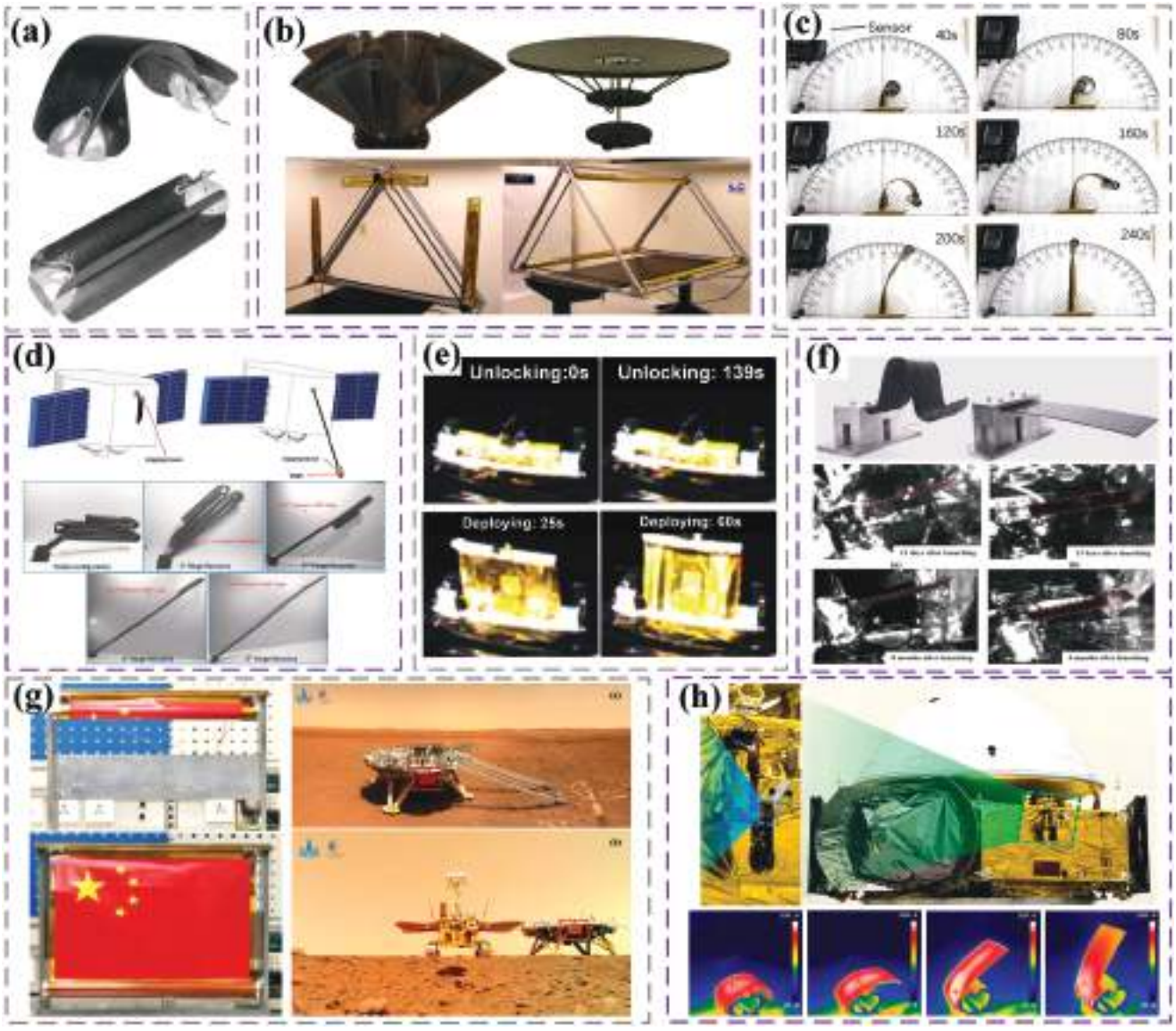

Figure 20. a,b) Lightweight hinge based on carbon fiber-reinforced SMPC. Reproduced with permission.[92] Copyright 2021,Amercian Institute of Aeronautics and Astronautics. c) Diagram of the recovery process. Reproduced with permission.[95] Copyright 2019, Elsevier. d) Rigid solar wing based on shape memory hinge. Reproduced with permission.[95c] Copyright 2021,Amercian Institute of Aeronautics and Astronautics. e) Recovery process of the LCCT. Reproduced with permission.[96b] Copyright 2020,Science press. f) On-orbit verification of SMEPC. Reproduced with permission.[95b] Copyright 2019, IOP Publishing Ltd. g) On-Mars qualification with the deployed Chinese national flag in a red frame. Reproduced with permission.[97] Copyright 2023, Elsevier.h) The space-deployable device was applied to the Tianwen-1 probe. Reproduced with permission.[96a] Copyright 2022,IOP Publishing Ltd.

physical manufacturing technologies. A double-layer film made of the carboxylic acid epoxy system was used by Lu et al. to construct a light-operated LCP crane with a high lifting capacity. **Figure** 21a depicts the telescopic arm returning to its extended position after turning off the NIR and UV light separately.[98] The direct manufacture of smart soft robots via 4D printing still confronts various hurdles, the key one being material and device compatibility. Jessica and colleagues inserted marketed iron-based magnetic micro-particles (MMP) within a unidirectional thermally activated SMP, resulting in a reconfigurable and remotely actuated soft robot.[99] The manufactured PU sheet responded to magnetic fields as well as light (Figure 21b). The authors thoroughly evaluated the magnetic field and photothermal response characteristics of the constructed shape memory cantilevers, flowers, and grippers, as well as their capacity to grasp small items. Feng et al. created a robot that can autonomously change from a rectangular shape to a helical structure and accomplish "wireless" self-propulsion when heated to 160 °C.[100] The 10 cm long soft robot displayed climbing abilities on slopes of about 20° and reached a top speed of 48 cm per minute on a horizontal surface (Figure 21c). By changing its proportions, the soft robot's pace may be altered. Figure 21d illustrates the universal approach Lv et al. suggested for incorporating multifunctional and programmable soft robots with conductive

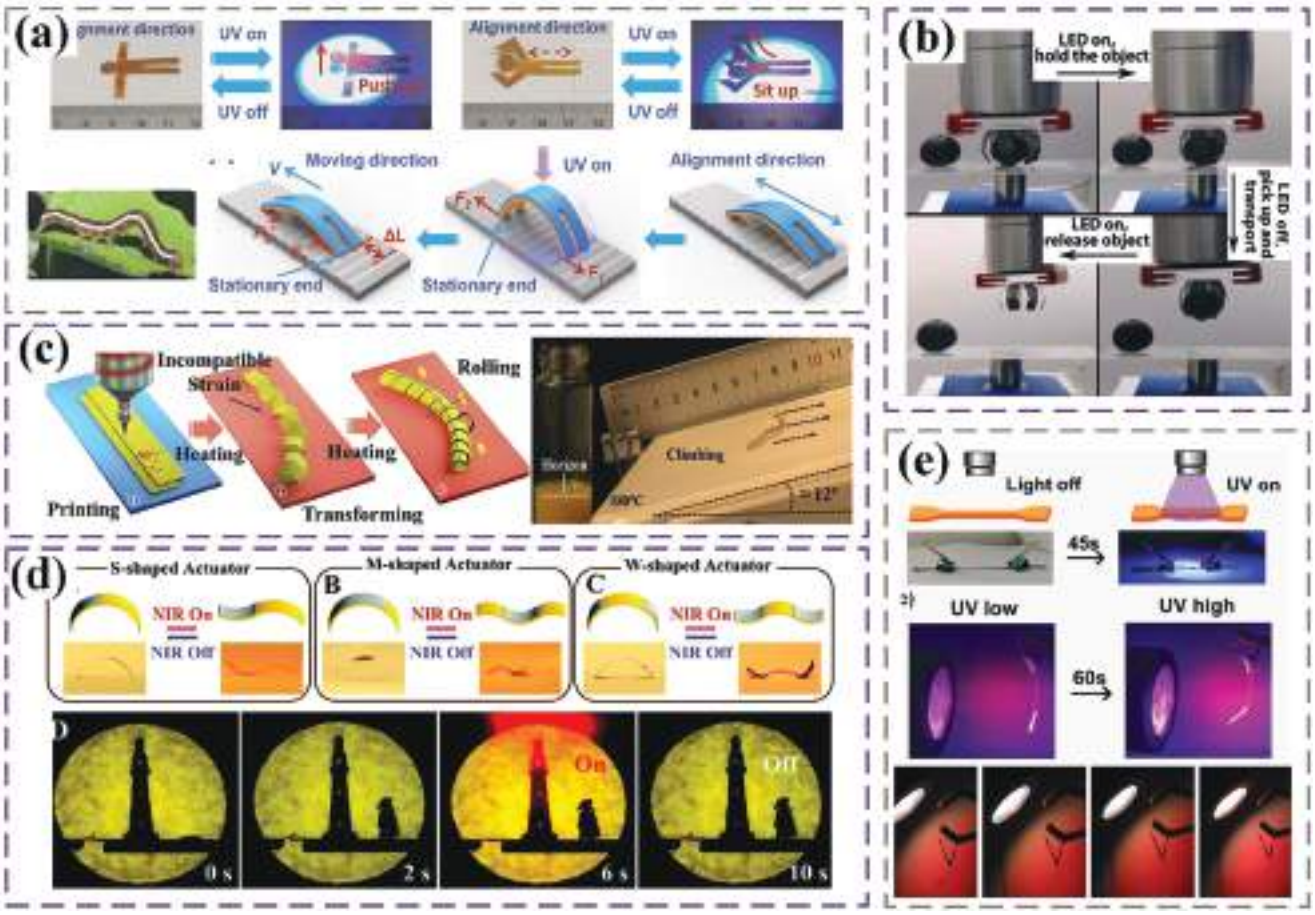

Figure 21. a) Caterpillar-inspired walker crawls forward during UV light cycles. Reproduced with permission.[98] Copyright 2018, Wiley-VCH. b) Grabbers can grab, transmit, and release SMP. Reproduced with permission.[99] Copyright 2019,American Association for the Advancement of Science. c) Thermal deformation of the sample and rolling process. Reproduced with permission.[100] Copyright 2021, Elsevier. d) NIR light-driven shape-programmable soft actuators. Reproduced with permission.[101] Copyright 2021, Royal Society of Chemistry. e) Artificial muscle activity induced by UV at 365 nm and NIR at 900 nm. Reproduced with permission.[102] Copyright 2021,

liquid metal (LM) and shape-transforming liquid crystal network (LCN).[101] The shape-programmable LM-LCN actuator combines the reversible shape deformation properties of LCN and the excellent thermal/electrical conductivity of LM, enabling both electrothermal and near-infrared (NIR) driving mechanisms. An innovative multifunctional programmable artificial muscle that combines the benefits of self-contained polymers and LCE by stacking azobenzene units together in a patch-sewn structure.[102] This muscle can deform when exposed to UV light and heal when exposed to infrared light in less than 30s (Figure 21e). The general principles of light-induced responses in elastomers were captured, validating the photoactuation by the related finite element analysis. Innovative nano-composite materials have potential uses in artificial muscles, soft robots, and smart skins, among other things.

5.3. Biomedical

Smart composite materials with 4D printing technology enable the quick production of intricate geometric tissue engineering scaffolds such as vascular stents, tracheal stents, cardiac occluders, bone tissue scaffolds, smart drug delivery systems, and surgical orthopedic devices (**Figure 22**). These discoveries reveal extensive application prospects in the realm of biomedicine. The dynamic and changing properties of 4D printed materials, in particular, have a high value in the minimally invasive implantation of tissue engineering scaffolds. They are conveniently kept in vitro in a compact temporary shape for minimally invasive surgery and interventional delivery. The scaffold can adjust and unfold in a regulated manner once it reaches the sick spot and is stimulated by external influences.

Li et al. organized the main achievements of 4D printing in the field of biomedicine. This article provides an overview of the progress of 4D printing, including its applications in vascular stents, tracheal stents, cardiac stents, and bone tissue stents.[103] Wei et al. created self-expanding vascular stents that can be driven without physical touch by incorporating magnetic Fe_3O_4 nanoparticles as functional particles into PLA. Vascular stents can be created specifically for each patient using direct-writing printing (**Figure 23a**).[104] According to Figure 23b, Lin et al. created a programmable 4D printed shape memory heart

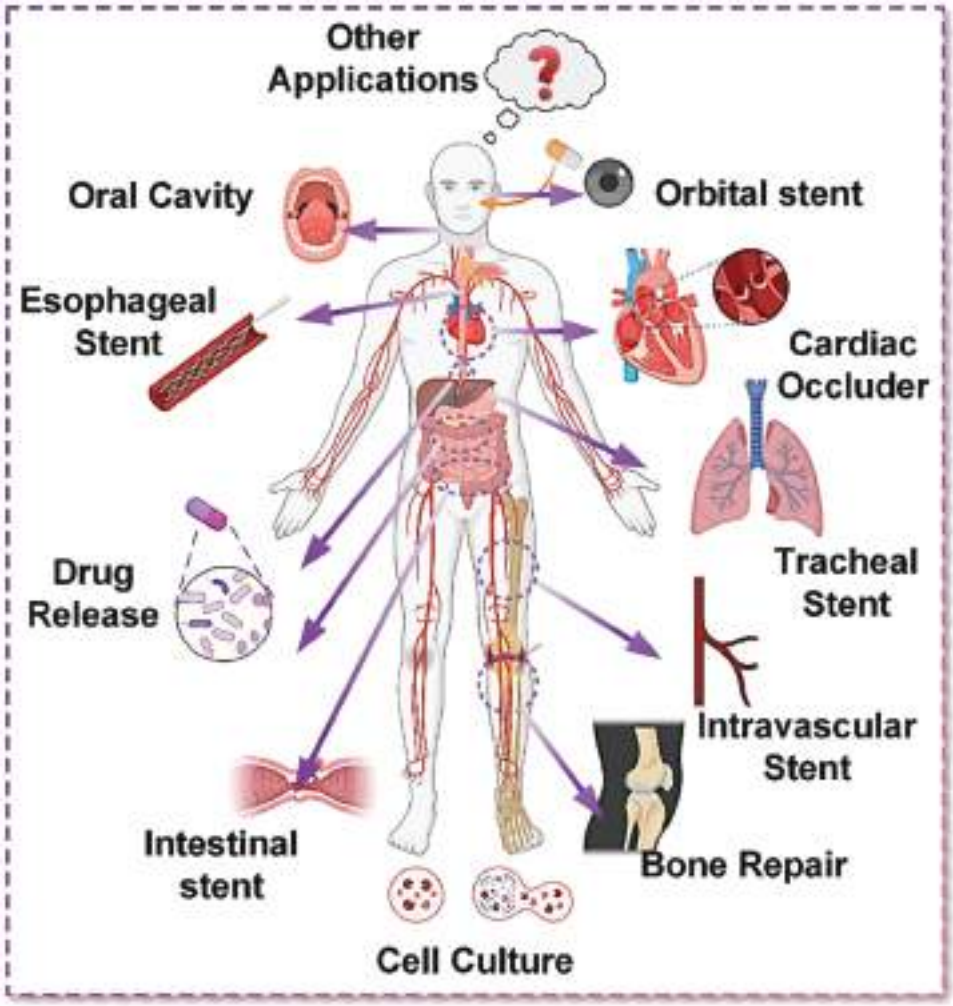

Figure 22. Application of 4D printing and AI to cardiovascular devices.

occluder, and after implanting it in rats, tissue slices showed the presence of degradation particles, demonstrating the occlude's biodegradability.[105] SMPU is used as a thermal responsive matrix and Mg is used as a photothermal and bioactive component to prepare near-infrared responsive scaffolds using low-temperature rapid prototyping (LT-RP) 3D printing technology (Figure 23c).[106] The scaffold exhibits a sustained photothermal effect, a strong mechanical structure, and uniform pores. Additionally, several in vitro and in vivo investigations have supported the bone repair-promoting effects of this scaffold, and it is anticipated that it will become a clinically useful bone regeneration method. For use in fused deposition modeling (FDM) printing, Zhang et al. synthesized PLA and PLA/Fe_3O_4 filaments (Figure 23d). These filaments were used to create porous structures for the healing of bone deformities. The porous structures can change from a temporary shape to their original shape when subjected to a magnetic field, enabling remote and contactless actuation.[107] Kim et al. proposed a novel 4D bioprinting strategy utilizing digital light processing (DLP) technology to print cell-laden hydrogel bilayer structures. The differential deformations of the bilayer hydrogel were utilized to construct complex trachea-like structures.[108] These structures were implanted into damaged rabbit trachea models to evaluate their applicability for tracheal regeneration and repair in vivo (Figure 23e)). Deng et al. created a SMPU for orbital support with CT visibility in ophthalmic treatment utilizing 4D printing. 4D printed orbital support with a honeycomb-like porous structure and a shape matching the orbital defect was created using biomimetic concepts and CT reconstruction techniques to offer precise and robust support for the orbital tissues, as shown in Figure 23f.[109]

5.4. Smart Textile

The surface tension, roughness, fiber form, twist, yarn fuzz, pore geometry, elasticity, and fabric morphology of textile substrates have a direct impact on the design, size, and print quality. Leist et al. created smart textiles by printing PLA (polylactic acid) and using FDM (fused deposition modeling) to incorporate shape memory characteristics into a mesh nylon fabric. According to **Figure** 24a, this fabric changes shape at 70 °C and

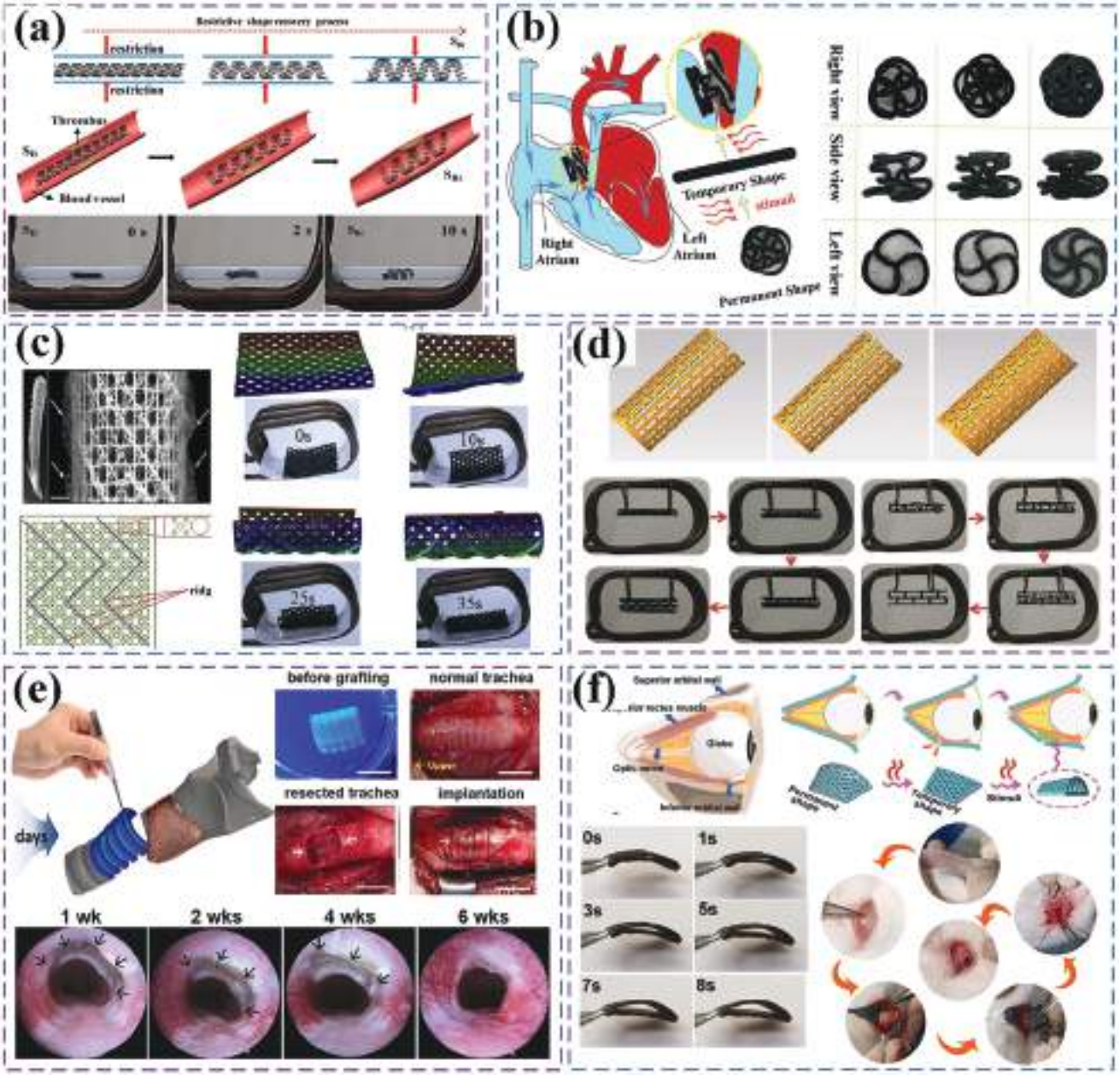

Figure 23. a) DW printing of a 4D scaffold ink and its potential biomedical application. Reproduced with permission.[104] Copyright 2017,American Chemical Society. b) The implantation process of shape memory occluder. Reproduced with permission.[105] Copyright 2019, Wiley-VCH. c) 4D printing of biomimetic tracheal stent. Reproduced with permission.[106] Copyright 2022, Elsevier. d) The magnetic drive shape of the 4D printing tracheal bracket is restored. Reproduced with permission.[107] Copyright 2019, Elsevier. e) 4D printing hydrogel like trachea structure. Reproduced with permission.[108] Copyright 2020, Elsevier. f) Procedure of the AHP stent implantation between the superior orbital wall and the eyeball in experimental rabbits. Reproduced with permission.[109] Copyright 2022, Elsevier.

returns to its original shape after 60 s.[110] It was also discussed how PLA and nylon fabric could be used to create smart textiles. When coupled with nylon fabric, PLA can maintain its thermal shape memory properties. The nylon fabric may be trained thermomechanically to take on a temporary shape and return to its permanent shape when heated. Smart textiles may be made by weaving traditional cotton fibers with soft robots using traditional weaving processes, successfully solving difficulties with drivability and durability. Figure 24b illustrates how DIW printing may be used to create long, flexible, and reversible LCE fibers.[111] The LCE fibers shrink when the fabric is heated to 80 °C, which causes voids to appear throughout the fabric. The resulting fibers' potential uses are shown by their 2 MPa modulus, 51% driving strain, and failure strain considerably above 100%. As seen in Figure 24c, Jang et al. created a hierarchically organized system based on keratin, which exhibits long-range

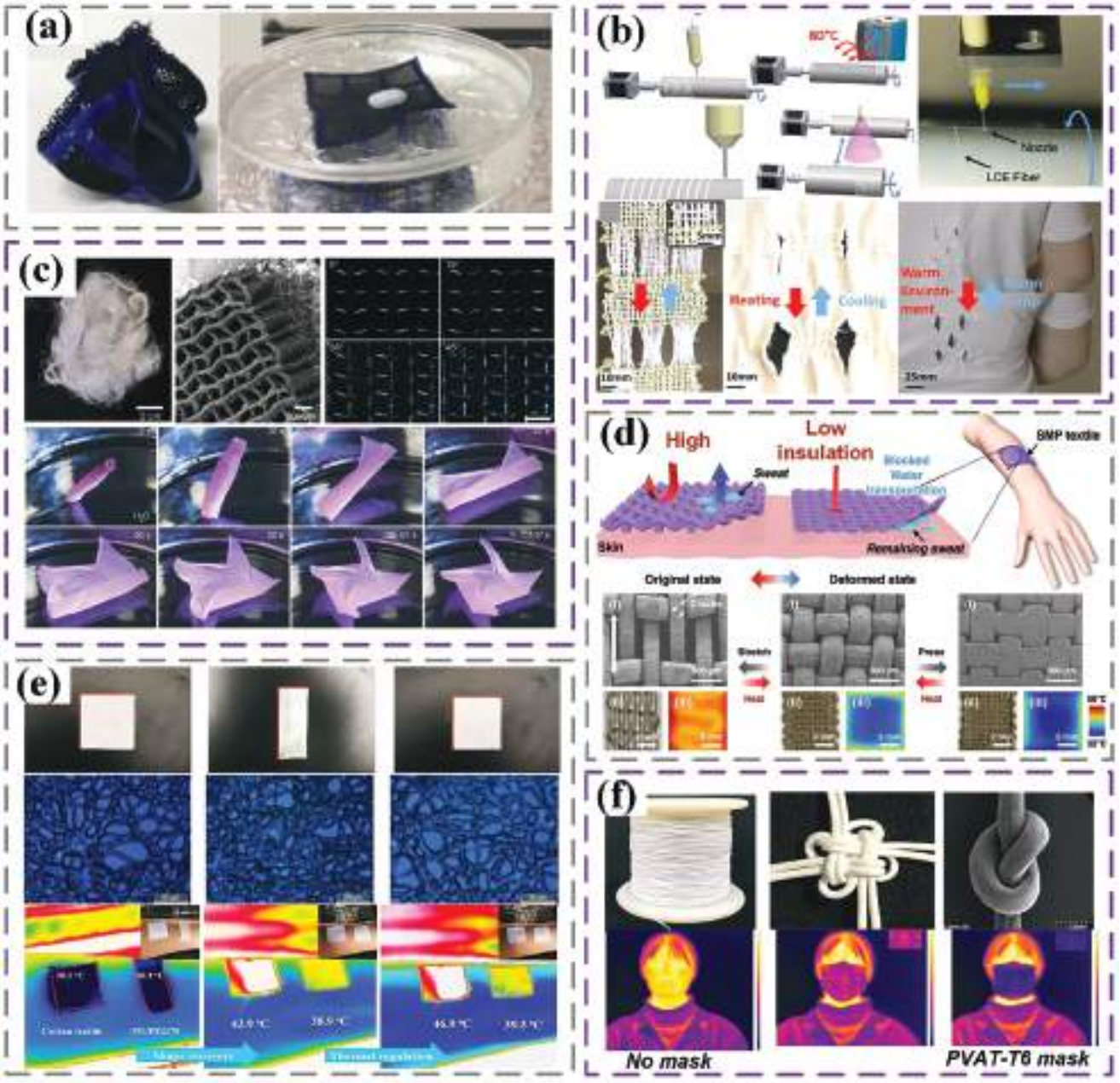

Figure 24. a)An example of using smart textiles for encapsulation applications. Reproduced with permission.[110] Copyright 2017, Taylor & Francis Ltd. b) Exercise-improved heat transfer and perspiration evaporation are demonstrated using the LCE smart shirt. Reproduced with permission.[111] Copyright 2019,American Chemical Society. c) WTSM effect in 3D architectures, which is illustrated with a star-shaped origami model. Reproduced with permission.[112] Copyright 2021, Royal Society of Chemistry. d) Design of an IR- and water-gating SMP textile. Reproduced with permission.[113] Copyright 2022, American Chemical Society. e) Photographs of the macroscale form fixation and shape recovery of the PU/PEG70 microporous membraneReproduced with permission.[70] Copyright 2021, Elsevier. f) The temperature of certain points on the infrared target with or without mask. Reproduced with permission.[114] Copyright 2021, Wiley-VCH.

molecular order and shape memory capabilities in response to hydration. High-strength SMPs with biocompatibility have been created through the investigation of substoichiometric reconstitution of keratin secondary structures, specifically the change from -helices to -sheets triggered by hydration.[112] In recent years, smart textile materials such as smart temperature regulation, shape memory, intelligent color change, and electronic information have been developing from wearing to wearing and in a wider range of fields, playing an important role in improving quality of life, improving labor conditions, and meeting the needs of special industries. The high concentration of proteins in the spinning fluid gives the fibers strength, making the spinning process flexible and trustworthy, and capable of producing continuous and uniform fibers (Figure 24d). The innovative material

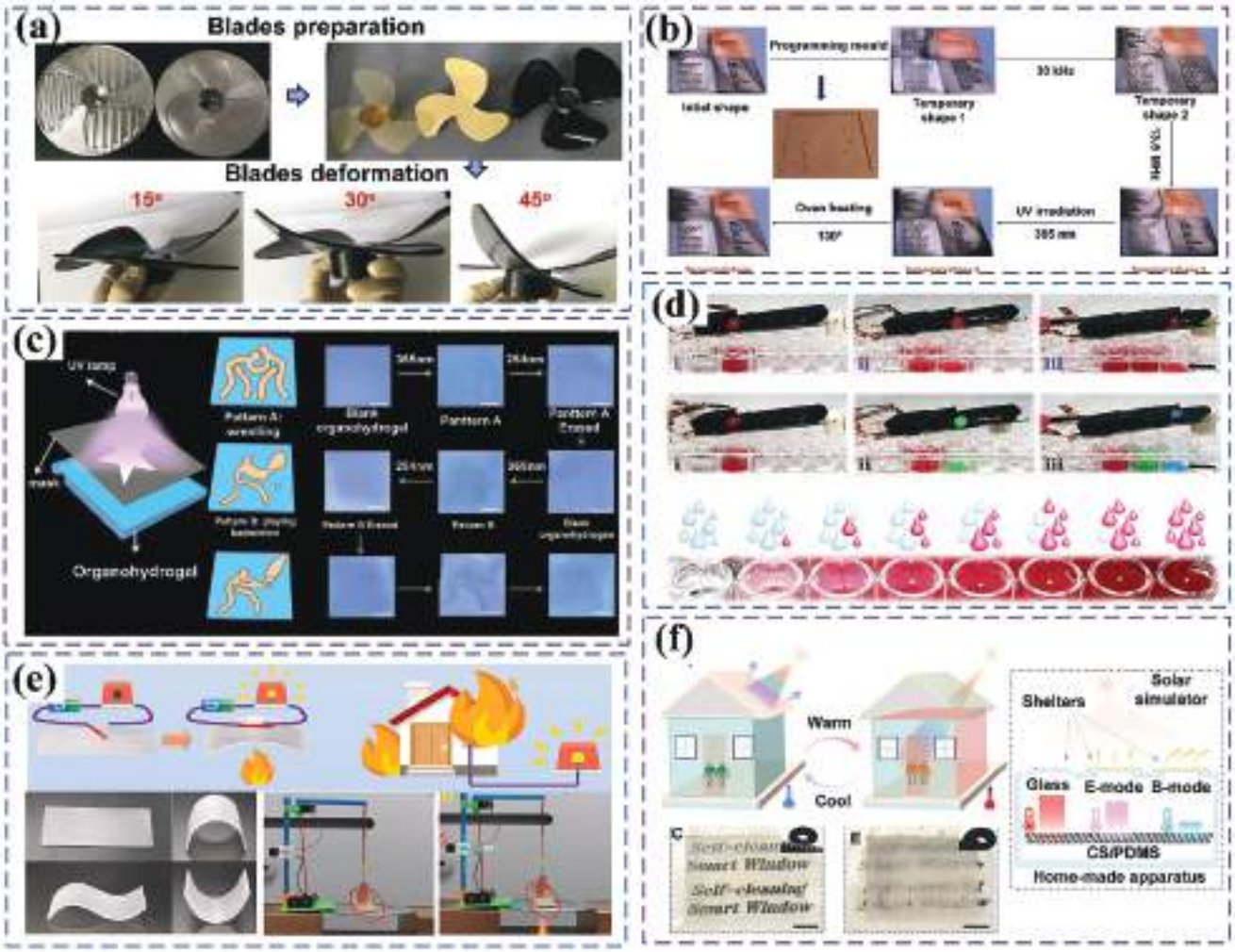

Figure 25. a) SMEPCs deformation and wind speed testing process. Reproduced with permission.[58] Copyright 2019,C. b) SMEP as an intelligent information carrier. Reproduced with permission.[115] Copyright 2017, American Chemical Society. c) Advanced double information encoding, encryption, and decryption of fluorescent organic hydrogels with shape memory properties. Reproduced with permission.[116] Copyright 2022, Wiley-VCH. d) By controlling the type and proportion of sliding sample droplets, the gradient concentration of the sample in the microporous plate hole is achieved. Reproduced with permission.[117] Copyright 2017, American Association for the Advancement of Science. e) Reconfigurable shape memory behavior and mechanism, as well as fire alarm driving function. Reproduced with permission.[118] Copyright 2022, Elsevier. f) The multifunctional characteristics of self-cleaning electronic control dual-mode intelligent windows and potential applications of films. Reproduced with permission.[119] Copyright 2023, Wiley-VCH.

allows for the sustainable sourcing of materials, enabling the development of biodegradable smart textiles. Stimulus-responsive smart textiles can efficiently safeguard human skin temperature from changing environmental conditions. A smart textile made of SMP fibers that can regulate water and IR transmission on human skin in an adaptable manner. An SMP fabric on a hot plate had its surface temperature successfully controlled by infrared images.[113] Additionally, the SMP fiber's structure, which can be employed to absorb perspiration from human skin, can open or close the directional transit of droplets. Figure 24e illustrates how an IR and water-gated smart textile offers a workable method for shielding human skin from alterations in the external environment. PU and polyethylene glycol (PEG) were used to make coaxial electrospun ultrafine fibers, with the PU serving as a supporting shell and the PEG serving as an energy storage core. Using coaxial electrospinning, PEG can create a "core–shell" structure inside microfibers.[70] PU/PEG membranes have outstanding cooling and drying performance due to their capacity to regulate temperature as well as their temperature-sensitive moisture permeability (Figure 24f). To improve wearer comfort in hot environments, they present a new approach to building smart textiles with dynamic thermal and moisture management functions. PVA solution was used to create continuous PVA aerogel fibers with aligned porosity morphology using freeze-thaw treatment and freeze-spinning procedures. The aerogel fiber spinning solution's spinnability is significantly enhanced by the freeze-thaw process, leading to the creation of continuous fibers. The link between PVA molecular chains and the aligned porosity structure gives the aerogel fibers ultrasoft and ultrastrong characteristics, resulting in superior weaving ability and appealing mechanical

Figure 26. Future trends of shape memory polymers and their composites.

qualities.[114] As demonstrated in Figure 24g, textiles made from this unique porous structured aerogel fibers perform remarkably well in terms of insulation.

5.5. Other Applications

SMPs offer a wide range of potential applications outside of aerospace, intelligent robots, and the medicinal sector. SMPs will expand prospects for innovation and development in these domains with further study and technological advancement, advancing future developments and applications. For example, fan motor blades can change shape automatically in reaction to environmental changes, and the shape of the blade will also affect how efficiently kinetic energy is converted, as shown in **Figure 25a**.[58] New anti-counterfeiting technologies, such as barcodes, QR codes, holograms, luminous materials, etc., have been the focus of many scientists in recent years. Due to its reactivity to UV light, variety of vivid hues, and various emission modes, luminescent materials have emerged as one of the top options for anticounterfeiting. Through the physical compounding of various response materials, Li et al. created four physically compatible function blocks based on SMEP, as seen in Figure 25b. As a system for intelligent information carriers, multiple codes can be lithographically created to disguise the initial code in response to new information under diverse stimuli.[115] Chen et al. disclosed a dual information encryption optical anticounterfeiting fluorescent oil/hydrogel with shape memory capabilities. The researchers developed an organic hydrogel by interpenetrating hydrophilic and hydrophobic polymers within a hydrogel network.[116] The anthracene unit can transition optically (Figure 25c). The monomer-dimer transition, which is initiated by 365 nm ultraviolet light, causes the fluorescent color of the organic hydrogel to change from blue to light yellow. This luminous organic hydrogel provides a new perspective on developing smart materials with encryption and decryption capabilities, which is critical for data security. Recently, numerous very smooth surfaces have been developed by infiltrating lubricating fluid into porous substrates, inspired by the unique smoothness of Nepenthes pitcher (Figure 25d).[117] Zhao et al. originally suggested a surface state control technique based on material SME, ultimately achieving intelligent control of droplets sliding on the surface. Transparent wood (TW) is made up of dignified skeletons submerged in transparent polymers (with a refractive index matching cellulose), which have drawn a lot of interest due to their high anisotropy, distinctive optical features, outstanding thermal insulation, superior mechanical strength, and potential, as shown in Figure 25e.[118] Shape reconfigurable TW has been constructed by integrating a poly thiocarbamate covalent adaptive network (PTU CAN) into a dignified wood (DW) scaffold. Due to its adjustable shape memory performance, it may be used as an intelligent driver for developing fire alarm systems. By giving conventional intelligent windows exceptional liquid-repellent and deicing features, Chen et al. created a Joule thermal sensitive, long-life, superhydrophobic, all solid-state, dimming, and temperature-controlled intelligent window (Figure 25f). This device exhibits versatility while also possessing anti-peep film characteristics.[119]

6. Summary and Outlook

SMPs enablethem to sense changes in the environment, process and analyze information, and achieve material/structure/function integration with self-sensing, self-deforming, self-healing, and self-learning functions. SMPs have vast potential in various fields like intelligent robotics, flexible electronics, intelligent sensors, and medical devices, and as technology continues to advance and deepen, the performance and application prospects of this material are expected to further improve and expand (**Figure 26**).

1) With the continuous development of both SMPs and artificial intelligence technology, their collaboration is poised to unleash astonishing potential in the future, as AI algorithms can optimize the manufacturing process of SMPs to predict

and adaptively adjust material properties, resulting in higher performance and adaptability. This will promote the progress of materials science and pave the way for product innovation.

2) Smart materials have become the cornerstone of contemporary industrial progress, finding use in critical domains including biomedicine, robotics, flexible electronics, artificial intelligence, and intelligent manufacturing. The use of SMPs will improve convenience and innovation in many businesses and people's lives, advancing both social progress and technological advancement. It is anticipated that these materials will have more viable application scenarios in the future due to the ongoing advancements in science and technology. The future intelligent society will profit greatly from the extensive study of smart materials on both an economic and social level.
3) By adjusting the crosslinking level crystal structure and adding various functional additives, the microstructure of SMPs can be optimized to realize multi-level deformation and multimode response functions, giving the substance the ability to respond to a variety of external stimuli like temperature, humidity, and light. This offers new opportunities for using SMPs in industries like flexible electronics and intelligent sensors, providing enormous potential for creating innovative materials.

Acknowledgements

The authors thank the National Key R&D Program of China (2022YFB3805700) and the National Natural Science Foundation of China(Grant No. 92271112) for the support of this work. [Correction added on January 2, 2024, after first online publication: Fenghua Zhang was assigned corresponding author in this version.]

Conflict of Interest

The authors declare no conflict of interest.

Author Contributions

L.L.: conceptualization, methodology, investigation, writing-review & editing. F.Z.: conceptualization, methodology, investigation, validation. L.W.: methodology, validation. Y.L.: conceptualization, supervision, writing-review & editing. J.L.: conceptualization, funding acquisition, supervision.

Keywords

application, composites, multiscale structures, shape memory polymer

Received: September 30, 2023
Revised: November 10, 2023
Published online: December 24, 2023

[1] a) J. Hu, Y. Zhu, H. Huang, J. Lu, *Prog. Polym. Sci.* **2012**, *37*, 1720; b) C. Liu, H. Qin, P. T. Mather, *J. Mater. Chem.* **2007**, *17*, 1543; c) T. Xie, *Polymer* **2011**, *52*, 4985.
[2] a) F. Xie, L. Huang, Y. Liu, J. Leng, *Polymer* **2014**, *55*, 5873; b) X. Xiao, D. Kong, X. Qiu, W. Zhang, F. Zhang, L. Liu, Y. Liu, S. Zhang, Y. Hu, J. Leng, *Macromolecules* **2015**, *48*, 3582.
[3] a) J. S. Leng, X. Lan, Y. J. Liu, S. Y. Du, W. M. Huang, N. Liu, S. J. Phee, Q. Yuan, *Appl. Phys. Lett.* **2008**, *92*, 014104; b) H. Lu, F. Liang, J. Gou, J. Leng, S. Du, *Smart Mater. Struct.* **2014**, *23*, 085034.
[4] a) X. Zhang, Q. Zhou, H. Liu, H. Liu, *Soft Matter* **2014**, *10*, 3748; b) A. Rose, Z. Zhu, C F. Madigan, T M. Swager, V. Bulovic, *Nature* **2005**, *434*, 876; c) H. Zhang, H. Xia, Y. Zhao, *J. Mater. Chem.* **2012**, *22*, 845; d) H.-X. Wang, X.-Y. Zhao, J.-Q. Jiang, Z.-T. Liu, Z.-W. Liu, G. Li, *ACS Appl. Mater. Interfaces* **2022**, *14*, 51244.
[5] a) L. Luo, F. Zhang, J. Leng, *Compos. Sci. Technol.* **2021**, *213*, 108899; b) N. G. Sahoo, Y. C. Jung, J. W. Cho, *Mater. Manuf. Processes* **2007**, *22*, 419.
[6] Y. Tan, Z. Liu, Z. Liu, J. Jiang, G. Li, *Chem. Eng. J.* **2023**, *454*, 140383.
[7] a) Y. Kai, Z. Zhang, Y. Liu, J. Leng, *Appl. Phys. Lett.* **2011**, *98*, 0741021; b) H. Lu, Y. Liu, J. Gou, J. Leng, S. Du, *Smart Mater. Struct.* **2010**, *19*, 075021; c) H. Guo, Y. Li, J. Zheng, J. Gan, L. Liang, K. Wu, M. Lu, *J. Appl. Polym. Sci.* **2015**, *40*, 132.
[8] a) T. Xiang, J. Hou, H. Xie, X. Liu, T. Gong, S. Zhou, *Nano Today* **2020**, *35*, 100980; b) H.-M. Chen, L. Wang, S.-B. Zhou, *Chin. J. Polym. Sci.* **2018**, *36*, 905; c) H. Xie, Ke-Ke Yang, Yu-Z Wang, *Prog. Polym. Sci.* **2019**, *95*, 32.
[9] a) A. Lendlein, A. M. Schmidt, R. Langer, *Proc. Natl. Acad. Sci. USA* **2001**, *98*, 842; b) A. Lendlein, A M. Schmidt, M. Schroeter, R. Langer, *J. Polym. Sci., Part A: Polym. Chem.* **2005**, *43*, 1369.
[10] a) J.-L. Hu, S. Mondal, *Polym. Int.* **2005**, *54*, 764; b) T. Calvo-Correas, N. Gabilondo, A. Alonso-Varona, T. Palomares, M. A Corcuera, A. Eceiza, *Eur. Polym. J.* **2016**, *78*, 253; c) C. Liu, H. Qin, P. T. Mather, *J. Mater. Chem.* **2007**, *17*, 1543; d) V. A. Beloshenko, V. N. Varyukhin, Y. V. Voznyak, *Prog. Chem.* **2005**, *74*, 265; e) L. Zhang, Z. Lin, Q. Zhou, S. Ma, Y. Liang, Z. Zhang, *Front. Mater. Sci.* **2020**, *14*, 177; f) Z. Yu, Y. Liu, M. Fan, X. Meng, B. Li, S. Zhang, *J. Polym. Sci.* **2010**, *48*, 951.
[11] W. Voit, T. Ware, R R. Dasari, P. Smith, L. Danz, D. Simon, S. Barlow, S R. Marder, K. Gall, *Adv. Funct. Mater.* **2010**, *20*, 162.
[12] T. D. Nguyen, C. M. Yakacki, P. D. Brahmbhatt, M. L Chambers, *Adv. Mater.* **2011**, *23*, 2778.
[13] S.-K. Ahn, P. Deshmukh, R M. Kasi, *Macromolecules* **2010**, *43*, 7330.
[14] J. Zhang, Y. Niu, C. Huang, L. Xiao, Z. Chen, K. Yang, Y. Wang, *Polym. Chem.* **2012**, *3*, 1390.
[15] J R. Capadona, K. Shanmuganathan, D J. Tyler, S J. Rowan, C. Weder, *Science* **2008**, *319*, 1370.
[16] C. Liu, S B. Chun, P T. Mather, L. Zheng, E H. Haley, E. B Coughlin, *Macromolecules* **2002**, *35*, 9868.
[17] X. Hu, J. Zhou, M. Vatankhah-Varnosfaderani, W. F. M. Daniel, Q. Li, A. P. Zhushma, A. V. Dobrynin, S. S. Sheiko, *Nat. Commun.* **2016**, *7*, 12919.
[18] W. Peng, G. Zhang, Q. Zhao, T. Xie, *Adv. Mater.* **2021**, *34*, 33.
[19] C. Ni, Di Chen, Yu Yin, X. Wen, X. Chen, C. Yang, G. Chen, Z. Sun, J. Wen, Y. Jiao, C. Wang, N. Wang, X. Kong, S. Deng, Y. Shen, R. Xiao, X. Jin, J. Li, X. Kong, Q. Zhao, T. Xie, *Nature* **2023**, *622*, 748.
[20] L. Luo, F. Zhang, Y. Liu, J. Leng, *Chem. Eng. J.* **2023**, *457*, 141228.
[21] S. Ma, Z. Jiang, M. Wang, L. Zhang, Y. Liang, Z. Zhang, L. Ren, L. Ren, *Bio-Des. Manuf.* **2021**, *4*, 867.
[22] Y. Zhou, Y. Yang, A. Jian, T. Zhou, G. Tao, L. Ren, J. Zang, Z. Zhang, *Compos. Sci. Technol.* **2022**, *227*, 109603.
[23] L. Ren, Z. Wang, L. Ren, Z. Han, X. L. Zhou, Z. Song, Q. Liu, *Composites, Part B* **2023**, *265*, 110959.
[24] W. He, X. Ming, Y. Xiang, C. Zhang, H. Zhu, Q. Zhang, S. Zhu, *ACS Appl. Mater. Interfaces* **2022**, *14*, 20132.
[25] H. Yan, Y. Wang, W. Shen, F. Li, G. Gao, T. Zheng, Z. Xu, S. Qian, C.-y. Chen, C. Zhang, G. Yang, T. Chen, *Adv. Funct. Mater.* **2022**, *34*, 32.
[26] C.-Y. Lo, Y. Zhao, C. Kim, Y. Alsaid, R. Khodambashi, M. Peet, R. Fisher, H. Marvi, S. Berman, D. Aukes, X. He, *Mater. Today* **2021**, *50*, 35.

[27] C. Wong, *Nat. Commun.* **2023**, *1*, 14.
[28] J. Liu, J. Li, S. Qiao, Z. Wang, P. Zhang, X. Fan, P. Cheng, Y.-S. Li, Y. Chen, Z. Zhang, *Angew. Chem., Int. Ed.* **2022**, *61*, e202212253.
[29] J. Peng, S. Xie, T. Liu, D. Wang, R. Ou, C. Guo, Q. Wang, Z. Liu, *Composites, Part B* **2022**, *242*, 110109.
[30] H. Xuan, Q. Guan, H. Tan, H. Zuo, L. Sun, Y. Guo, L. Zhang, R. E. Neisiany, Z. You, *ACS Nano* **2022**, *16*, 16954.
[31] Z. Ren, Z. Ren, Z. Zhang, T. Buonassisi, J. Li, *Nat. Rev. Mater.* **2023**, *8*, 563.
[32] G X. Gu, C.-T. Chen, D J. Richmond, M J. Buehler, *Mater. Horiz.* **2018**, *5*, 939.
[33] W. Trehern, R. Ortiz-Ayala, K. C. Atli, R. Arroyave, I. Karaman, *Acta Mater.* **2022**, *228*, 117751.
[34] D. S. Ibarra, J. Mathews, F. Li, H. F. Lu, G. Q. Li, J. Y. Chen, *Polymer* **2022**, *261*, 125395.
[35] A. Zolfagharian, L. Durran, S. Gharaie, B. Rolfe, A. Kaynak, M. Bodaghi, *Sens. Actuators, A* **2021**, *328*, 112774.
[36] D. S. Ibarra, J. Mathews, F. Li, H. F. Lu, G. Q. Li, J. Y. Chen, *Polymer* **2022**, *261*, 15.
[37] A. Shafe, C. D. Wick, A. J. Peters, X. Y. Liu, G. Q. Li, *Polymer* **2022**, *242*, 124577.
[38] C. Yan, X. M. Feng, C. Wick, A. Peters, G. Q. Li, *Polymer* **2021**, *214*, 123351.
[39] T. Liu, T. Zhou, Y. Yao, F. Zhang, L. Liu, Y. Liu, J. Leng, *Composites, Part A* **2017**, *100*, 20.
[40] Q. Ze, X. Kuang, S. Wu, J. Wong, S. M. Montgomery, R. Zhang, J. M. Kovitz, F. Yang, H. J. Qi, R. Zhao, *Adv. Mater.* **2020**, *32*, 1906657.
[41] A. Belmonte, M. Pilz Da Cunha, K. Nickmans, A P. H. J. Schenning, *Adv. Opt. Mater.* **2020**, *8*, 2000054.
[42] Q. Guo, C. J. Bishop, R. A. Meyer, D. R. Wilson, L. Olasov, D. E. Schlesinger, P. T. Mather, J. B. Spicer, J. H. Elisseeff, J. J. Green, *ACS Appl. Mater. Interfaces* **2018**, *10*, 13333.
[43] M. Liu, M. Fan, S. Zhu, W. Liu, L. Yang, D. Ge, *J. Mater. Chem. C* **2023**, *11*, 4570.
[44] Y. Liu, X. Wei, X. He, J. Yao, R. Tan, P. Chen, B. Yao, J. Zhou, Z. Yao, *Adv. Funct. Mater.* **2023**, *33*, 2211352.
[45] P. Bhuyan, Y. Wei, D. Sin, J. Yu, C. Nah, K.-U. Jeong, M. D. Dickey, S. Park, *ACS Appl. Mater. Interfaces* **2021**, *13*, 28916.
[46] W. Liu, H. Chen, M. Ge, Q.-Q. Ni, Q. Gao, *Mater. Des.* **2018**, *143*, 196.
[47] W. Zhao, C. Gao, H. Sang, J. Xu, C. Wang, Y. Wu, *RSC Adv.* **2016**, *6*, 52982.
[48] Y. Zhu, J. Hu, H. Luo, R J. Young, L. Deng, S. Zhang, Y. Fan, G. Ye, *Soft Matter* **2012**, *8*, 2509.
[49] Z. Wang, J. Liu, J. Guo, X. Sun, L. Xu, *Polymers* **2017**, *11*, 9.
[50] M. Park, Y. Kim, J Ok Hwang, J. K. Park, *Carbon Lett.* **2019**, *29*, 219.
[51] Y. Wang, Z. Chen, J. Niu, Y. Shi, J. Zhao, J. Ye, W. Tian, *Front. Chem.* **2020**, *8*, 322.
[52] C B. Cooper, S. Nikzad, H. Yan, Y. Ochiai, J.-C. Lai, Z. Yu, G. Chen, J. Kang, Z. Bao, *ACS Cent. Sci.* **2021**, *7*, 1657.
[53] J. Yuan, W. Neri, C. Zakri, P. Merzeau, K. Kratz, A. Lendlein, P. Poulin, *Science* **2019**, *365*, 155.
[54] S. Park, N. Baugh, H. K. Shah, D. P. Parekh, I. D. Joshipura, M. D. Dickey, *Adv. Sci.* **2019**, *6*, 1901579.
[55] H. Venkatesan, J. Chen, H. Liu, Y. Kim, S. Na, W. Liu, J. Hu, *Mater. Chem. Front.* **2019**, *3*, 2472.
[56] K. Y. Chun, S. H. Kim, M. K. Shin, C. H. Kwon, J. Park, Y. T. Kim, G. M. Spinks, M. D. Lima, C. S. Haines, R. H. Baughman, S. J. Kim, *Nat. Commun.* **2014**, *5*, 3322.
[57] M. Q. Chen, Y. D. Cui, Y. X. Wang, C. Y. Chang, *Chem. Eng. J.* **2023**, *453*, 139893.
[58] Y. Liu, Y. Guo, J. Zhao, X. Chen, H. Zhang, G. Hu, X. Yu, Z. Zhang, *Compos. Sci. Technol.* **2019**, *177*, 49.
[59] K. Gall, M. Mikulas, N A. Munshi, F. Beavers, M. Tupper, *J. Intell. Mater. Syst. Struct.* **2000**, *11*, 877.
[60] R. Ali, S. Iannace, L. Nicolais, *Compos. Sci. Technol.* **2003**, *63*, 2217.
[61] J. Yao, T. Li, S. Ma, G. Qian, G. Song, J. Zhang, H. Zhou, G. Liu, *Smart Mater. Struct.* **2020**, *11*, 29.
[62] J. Deitzel, *Polymer* **2002**, *43*, 1025.
[63] a) R. G. Flemming, C. J. Murphy, G. A. Abrams, S. L. Goodman, P. F. Nealey, *Biomaterials* **1999**, *20*, 573; b) F. R. Lamastra, D. Puglia, M. Monti, A. Vella, L. Peponi, J. M. Kenny, F. Nanni, *Chem. Eng. J.* **2012**, *195*, 140; c) M. P. Arrieta, A. Diez Garcia, D. Lopez, S. Fiori, L. Peponi, *Nanomaterials* **2019**, *9*, 346; d) E D. Boland, B D. Coleman, C P. Barnes, D G. Simpson, G E. Wnek, G L. Bowlin, *Acta Biomater.* **2005**, *1*, 115.
[64] a) D. Li, Y. Xia, *Adv. Mater.* **2004**, *16*, 1151; b) Y. M. Shin, M. M. Hohman, M. P. Brenner, G. C. Rutledge, *Appl. Phys. Lett.* **2001**, *78*, 1149; c) G. Yang, X. Li, Y. He, J. Ma, G. Ni, S. Zhou, *Prog. Polym. Sci.* **2018**, *81*, 80.
[65] F. Zhang, Z. Zhang, Y. Liu, W. Cheng, Y. Huang, J. Leng, *Composites, Part A* **2015**, *76*, 54.
[66] F. H. Zhang, Z. C. Zhang, C. J. Luo, I.-T. Lin, Y. Liu, J. Leng, S K. Smoukov, *J. Mater. Chem. C* **2015**, *3*, 11290.
[67] F. Zhang, Z. Zhang, Y. Liu, H. Lu, J. Leng, *Smart Mater. Struct.* **2013**, *22*, 085020.
[68] W. Wei, P. Zhang, F. Cao, J. Liu, K. Qian, D. Pan, Y. Yao, W. Li, *Chem. Eng. J.* **2022**, *446*, 137135.
[69] Lu Wang, J. Ma, T. Guo, F. Zhang, A. Dong, S. Zhang, Y. Liu, H. Yuan, J. Leng, *Adv. Fiber Mater.* **2023**, *5*, 632.
[70] W. Feng, Y.-s. Zhang, Y.-w. Shao, T. Huang, N. Zhang, J.-h. Yang, X.-d. Qi, Y. Wang, *Eur. Polym. J.* **2021**, *145*, 110245.
[71] Y. Bai, Z. Zhou, Q. Zhu, S. Lu, Y. Li, L. Ionov, *Carbohydr. Polym.* **2023**, *313*, 120898.
[72] a) X. Xin, L. Liu, Y. Liu, J. Leng, *Adv. Funct. Mater.* **2020**, *30*, 2004226; b) X. Xin, L. Liu, Y. Liu, J. Leng, *Adv. Funct. Mater.* **2022**, *32*, 2107795.
[73] N. Li, W. Zhao, F. Li, L. Liu, Y. Liu, J. Leng, *Matter* **2023**, *6*, 940.
[74] C. Yang, M. Boorugu, A. Dopp, J. Ren, R. Martin, D. Han, W. Choi, H. Lee, *Mater. Horiz.* **2019**, *6*, 1244.
[75] B. Li, C. Zhang, F. Peng, W. Wang, B. D. Vogt, K. T. Tan, *J. Mater. Chem. C* **2021**, *9*, 1164.
[76] G. Liu, Y. Zhao, G. Wu, J. Lu, *Sci. Adv.* **2018**, *8*, 4.
[77] W. Zhao, N. Li, X. Liu, L. Liu, C. Yue, C. Zeng, Y. Liu, J. Leng, *Nano Energy* **2023**, *115*, 108697.
[78] X. Liu, M. Wei, Q. Wang, Y. Tian, J. Han, H. Gu, H. Ding, Q. Chen, K. Zhou, Z. Gu, *Adv. Mater.* **2021**, *33*, 2100332.
[79] a) C. Zeng, L. Liu, W. Bian, J. Leng, Y. Liu, *Compos. Struct.* **2022**, *280*, 114952; b) C. Zeng, L. Liu, W. Bian, Y. Liu, J. Leng, *Composites, Part B* **2020**, *194*, 108034.
[80] K. Dong, Y. Wang, Z. Wang, W. Qiu, P. Zheng, Y. Xiong, *Composites, Part A* **2023**, *169*, 107529.
[81] K. Dong, H. Ke, M. Panahi-Sarmad, T. Yang, X. Huang, X. Xiao, *Mater. Des.* **2021**, *198*, 109303.
[82] R. Xing, J. Yang, D. Zhang, W. Gong, T V. Neumann, M. Wang, R. Huang, J. Kong, W. Qi, M D. Dickey, *Matter* **2023**, *6*, 2248.
[83] X.-B. Wang, X.-F. Jiang, Y. Bando, *Bull. Chem. Soc. Jpn.* **2019**, *92*, 245.
[84] R. Abedin, J. Konlan, X. Feng, P. Mensah, G. Li, *Smart Mater. Struct.* **2022**, *31*, 095009.
[85] J. Yang, X. Shen, W. Yang, J.-K. Kim, *Prog. Mater. Sci.* **2023**, *133*, 101054.
[86] A. Idowu, T. Thomas, J. Bustillos, B. Boesl, A. Agarwal, *Polymers* **2023**, *15*, 2903.
[87] R. Zhao, S. Kang, C. Wu, Z. Cheng, Z. Xie, Y. Liu, D. Zhang, *Adv. Sci.* **2023**, *10*, 8.
[88] P. Liu, H. Lai, X. Luo, Q. Xia, D. Zhang, Z. Cheng, Y. Liu, L. Jiang, *ACS Nano* **2020**, *14*, 14047.

[89] J. Chen, W.-j. Jiang, Z. Zeng, D.-x. Sun, X.-d. Qi, J.-h. Yang, Y. Wang, *Chem. Eng. J.* **2023**, *466*, 143373.
[90] J. Rong, J. Zhou, Y. Zhou, C. Hu, L. Li, W. Guo, *Small* **2022**, *51*, 18.
[91] L. Zhao, L. Wang, J. Shi, X. Hou, Qi Wang, Y. Zhang, Y. Wang, N. Bai, J. Yang, J. Zhang, Bo Yu, C. F. Guo, *ACS Nano* **2021**, *15*, 5752.
[92] J. Lin, C. Knoll, C. Willey, in *47th AIAA/ASME/ASCE/AHS/ASC Structures, Structural Dynamics, and Materials Conf. 7th*, AIAA, Reston, VA **2006**.
[93] J. Leng, X. Wu, Y. Liu, *Smart Mater. Struct.* **2009**, *18*, 095031.
[94] H. Lu, K. Yu, Y. Liu, J. Leng, *Smart Mater. Struct.* **2010**, *19*, 065014.
[95] a) Z. Liu, Q. Li, W. Bian, X. Lan, Y. Liu, J. Leng, *Compos. Struct.* **2019**, *223*, 110936; b) F. Li, L. Liu, X. Lan, C. Pan, Y. Liu, J. Leng, Q. Xie, *Smart Mater. Struct.* **2019**, *28*, 075023; c) X. Lan, L. Liu, C. Pan, F. Li, Z. Liu, G. Hou, J. Sun, W. Dai, L. Wang, H. Yue, Y. Liu, J. Leng, X. Zhong, Y. Tang, *AIAA J.* **2021**, *59*, 2200.
[96] a) D. Zhang, L. Liu, P. Xu, Y. Zhao, Q. Li, X. Lan, F. Zhang, L. Wang, X. Wan, X. Zou, C. Zeng, X. Xin, W. Dai, Y. Li, Y. He, Y. Liu, J. Leng, *Smart Mater. Struct.* **2022**, *11*, 31; b) X. Lan, L. Liu, F. Zhang, Z. Liu, L. Wang, Q. Li, F. Peng, S. Hao, W. Dai, X. Wan, Y. Tang, M. Wang, Y. Hao, Y. Yang, C. Yang, Y. Liu, J. Leng, *Sci. China:Technol. Sci.* **2020**, *63*, 1436.
[97] C. Zeng, L. Liu, Y. Du, M. Yu, X. Xin, P. Xu, F. Li, L. Wang, F. Zhang, Y. Liu, J. Leng, *Compos. Commun.* **2023**, *42*, 101690.
[98] X. Lu, H. Zhang, G. Fei, B. Yu, X. Tong, H. Xia, Y. Zhao, *Adv. Mater.* **2018**, *30*, 1706597.
[99] J. A. C. Liu, J. H. Gillen, S. R. Mishra, B. A. Evans, J. B. Tracy, *Sci. Adv.* **2019**, *5*, 2000147.
[100] F. Zhai, Y. Feng, Z. Li, Y. Xie, J. Ge, H. Wang, W. Qiu, W. Feng, *Matter* **2021**, *4*, 3313.
[101] P. Lv, X. Yang, H. K. Bisoyi, H. Zeng, X. Zhang, Y. Chen, P. Xue, S. Shi, A. Priimagi, L. Wang, W. Feng, Q. Li, *Mater. Horiz.* **2021**, *8*, 2475.
[102] C. Chen, Y. Liu, X. He, H. Li, Y. Chen, Y. Wei, Y. Zhao, Y. Ma, Z. Chen, Xu Zheng, H. Liu, *Chem. Mater.* **2021**, *33*, 987.
[103] Y. Li, F. Zhang, Y. Liu, J. Leng, *Sci. China: Technol. Sci.* **2020**, *63*, 545.
[104] H. Wei, Q. Zhang, Y. Yao, L. Liu, Y. Liu, J. Leng, *ACS Appl. Mater. Interfaces* **2017**, *9*, 876.
[105] C. Lin, J. Lv, Y. Li, F. Zhang, J. Li, Y. Liu, L. Liu, J. Leng, *Adv. Funct. Mater.* **2019**, *29*, 1906569.
[106] Y. Zhang, C. Li, W. Zhang, J. Deng, Y. Nie, X. Du, L. Qin, Y. Lai, *Bioact. Mater.* **2022**, *16*, 218.
[107] F. Zhang, L. Wang, Z. Zheng, Y. Liu, J. Leng, *Composites, Part A* **2019**, *125*, 105571.
[108] S. H. Kim, Y. B. Seo, Y. K. Yeon, Y. J. Lee, H. S. Park, M. T. Sultan, J. M. Lee, J. S. Lee, O. J. Lee, H. Hong, H. Lee, O. Ajiteru, Y. J. Suh, S.-H. Song, K.-H. Lee, C. H. Park, *Biomaterials* **2020**, *260*, 120281.
[109] Y. Deng, B. Yang, F. Zhang, Y. Liu, J. Sun, S. Zhang, Y. Zhao, H. Yuan, J. Leng, *Biomaterials* **2022**, *291*, 121886.
[110] S K. Leist, D. Gao, R. Chiou, J. Zhou, *Virtual Phys. Prototyping* **2017**, *12*, 290.
[111] D. J. Roach, C. Yuan, X. Kuang, V. C.-F. Li, P. Blake, M. L. Romero, I. Hammel, K. Yu, H. J. Qi, *ACS Appl. Mater. Interfaces* **2019**, *11*, 19514.
[112] D. Jang, C. B. Thompson, S. Chatterjee, L. T. J. Korley, *Mol. Syst. Des. Eng.* **2021**, *6*, 1003.
[113] A. Choe, Y. Kwon, Y.-E. Shin, J. Yeom, J. Kim, H. Ko, *ACS Appl. Mater. Interfaces* **2022**, *14*, 55217.
[114] Y. Liu, Y. Zhang, X. Xiong, P. Ge, J. Wu, J. Sun, J. Wang, Q. Zhuo, C. Qin, L. Dai, *Macromol. Mater. Eng.* **2021**, *306*, 2100399.
[115] W. Li, Y. Liu, J. Leng, *ACS Appl. Mater. Interfaces* **2017**, *9*, 44792.
[116] H. Shang, X. Le, Y. Sun, F. Shan, S. Wu, Y. Zheng, D. Li, D. Guo, Q. Liu, T. Chen, *Adv. Opt. Mater.* **2022**, *10*, 2200608.
[117] J. Wang, L. Sun, M. Zou, W. Gao, C. Liu, L. Shang, Z. Gu, Y. Zhao, *Sci. Adv.* **2017**, *3*, e170004.
[118] K. Wang, T. Zhang, C. Li, X. Xiao, Y. Tang, X. Fang, H. Peng, X. Liu, Y. Dong, Y. Cai, D. Tian, Y. Li, J. Li, *Composites, Part B* **2022**, *246*, 110260.
[119] C. Chen, H. Yao, S. Guo, Z. Lao, Y. Xu, S. Li, S. Wu, *Adv. Funct. Mater.* **2023**, *3*, 33.

Lan Luo is pursuing a Ph.D. in materials science at the Center for Smart Materials and Structures at Harbin Institute of Technology (HIT) in China. Currently, she is focusing on shape memory polymer molecular structure design, multifunctional composites, and their applications.

Fenghua Zhang is an associate professor in Center for Smart Materials and Structures at Harbin Institute of Technology (HIT), China. She obtained her Ph.D. degree in the field of materials at HIT in 2017. From 2014 to 2016, she as a visiting student did her research work at the University of Cambridge supported by CSC. She has published more than 80 SCI scientific papers. Her research interests are focusing on shape memory polymers and their composites, including shape memory polymers with nano/microstructures, 4D printed smart materials and structures for biomedical applications, stimuli methods, and multifunctional composite material.

Linlin Wang is an assistant researcher at Harbin Institute of Technology. She received his Ph.D. degree in materials science at Harbin Institute of Technology in December 2022. Her current research focuses on functional shape memory polymers and composites and advanced manufacturing innovation for aerospace applications.

Yanju Liu is a professor in the Department of Aerospace Science and Mechanics at the Harbin Institute of Technology (HIT), China. From 1999 to 2003, she was a research fellow at Nanyang Technological University and Newcastle University. She was invited to serve as an associate editor of the Journal of Smart Materials and Structures, a committee member of APCSNM, and a committee member of SAMPE. She is working on smart materials and structures, including electrorheological and magnetorheological fluids, electroactive polymers, and shape memory polymers and their nanocomposites. She has authored or co-authored over 200 scientific papers in different journals.

Jinsong Leng is a full professor and director of Center for Smart Materials and Structures at Harbin Institute of Technology, China. His research interests cover smart materials and structures. He served as the vice president of the International Committee on Composite Materials (ICCM). He is elected as the academician of the Chinese Academy of Sciences, a foreign member of Academia Europaea, a member of the European Academy of Science and Arts, a world fellow of ICCM, a fellow of AAAS, fellow of SPIE, a fellow of the Institute of Physics (IOP), fellow of Royal Aeronautical Society (RAeS), fellow of IMMM and associate fellow of AIAA.